Glycoconj J (2009) 26:1151–1169
DOI 10.1007/s10719-009-9236-y

Disease-associated glycosylated molecular variants of human C-reactive protein activate complement-mediated hemolysis of erythrocytes in tuberculosis and Indian visceral leishmaniasis

Waliza Ansar · Sumi Mukhopadhyay · SK. Hasan Habib · Shyamasree Basu · Bibhuti Saha · Asish Kumar Sen · CN. Mandal · Chitra Mandal

Received: 23 July 2008 / Revised: 28 February 2009 / Accepted: 23 March 2009 / Published online: 5 June 2009

Abstract Human C-reactive protein (CRP), as a mediator of innate immunity, removed damaged cells by activating the classical complement pathway. Previous studies have successfully demonstrated that CRPs are differentially induced as glycosylated molecular variants in certain pathological conditions. Affinity-purified CRPs from two most prevalent diseases in India *viz*. tuberculosis (TB) and *visceral leishmaniasis* (VL) have differential glycosylation in their sugar composition and linkages. As anemia is a common manifestation in TB and VL, we assessed the contributory role of glycosylated CRPs to influence hemolysis via CRP-complement-pathway as compared to healthy control subjects. Accordingly, the specific binding of glycosylated CRPs with erythrocytes was established by flow-cytometry and ELISA. Significantly, deglycosylated CRPs showed a 7–8-fold reduced binding with erythrocytes confirming the role of glycosylated moieties. Scatchard analysis revealed striking differences in the apparent binding constants (10^4–$10^5 M^{-1}$) and number of binding sites (10^6–10^7sites/erythrocyte) for CRP on patients' erythrocytes as compared to normal. Western blotting along with immunoprecipitation analysis revealed the presence of distinct molecular determinants on TB and VL erythrocytes specific to disease-associated CRP. Increased fragility, hydrophobicity and decreased rigidity of diseased-erythrocytes upon binding with glycosylated CRP suggested membrane damage. Finally, the erythrocyte-CRP binding was shown to activate the CRP-complement-cascade causing hemolysis, even at physiological concentration of CRP (10 μg/ml). Thus, it may be postulated that CRP have a protective role towards the clearance of damaged-erythrocytes in these two diseases.

Keywords Glycosylated C-reactive protein · Damaged-erythrocytes · Complement-mediated hemolysis · Tuberculosis · Visceral leishmaniasis

W. Ansar · S. Mukhopadhyay · SK. H. Habib · S. Basu · C. Mandal (✉)
Infectious disease and Immunology Division,
Indian Institute of Chemical Biology,
4, Raja S.C Mullick Road, Jadavpur,
Kolkata 700 032, India
e-mail: cmandal@iicb.res.in
e-mail: chitra_mandal@yahoo.com

CN. Mandal
Structural Biology and Bioinformatics Division,
Indian Institute of Chemical Biology,
4, Raja S.C Mullick Road, Jadavpur,
Kolkata 700 032, India

A. K. Sen
Department of Organic Chemistry,
Indian Institute of Chemical Biology,
4, Raja S.C Mullick Road, Jadavpur,
Kolkata 700 032, India

B. Saha
Department of Tropical Medicine,
School of Tropical Medicine,
Chittaranjan Avenue,
Kolkata 700073, India

Present Address:
S. Mukhopadhyay
School of Tropical Medicine,
Kolkata, India

Abbreviations

αGalNAc	alpha-*N*-acetyl Galactosamine
αGlcNAc	alpha-*N*-acetyl Glucosamine
α-L-Fuc	alpha-L-fucose
ABTS	2, 2′-azino-bis (3-ethylbenzthiazole-6-sulfonic acid)
ANS	8-anilino-1-napthalenesulfonic acid
BSA	Bovine Serum Albumin
$CaCl_2$	Calcium Chloride
CHAPS	3-(3-cholamidopropyl) dimethylammonio)-1-propanesulfonic acid
Con A	Concanavalin A
CRP	C-reactive protein
CRP_{TB} and CRP_{VL}	Purified CRP from patients with TB and VL
CRP_{Sigma}	CRP purified from human plasma purchased from Sigma Chemical Company
DAB	3, 3-diaminobenzidine
DBA	*Dolichos biflorus* agglutinin
DIG	Dioxigenin
DPH	1,6-diphenyl-1, 3, 5-hexatriene
DSA	*Datura stramonium* agglutinin
E	Erythrocytes
E_{TB}, E_{VL} and E_N	Erythrocytes from TB, VL and normal (N) individuals
EDTA	Ethylene diamine tetra acetic acid
ELISA	Enzyme-linked immunosorbent assay
FACS	Fluorescence activated cell sorter
FITC	Fluorescein isothiocynate
GLC	Gas liquid chromatography
GNA	*Galanthus nivalis* agglutinin
GVB	Gelatin-veronal-buffered
HRP	Horseradish peroxidase
I	Iodine
IEF	Isoelectric focussing
IgG	Immunoglobulin G
kDa	kilo Dalton
MAA	*Maackia amurensis* agglutinin
MAC	Membrane attack complex
NaCl	Sodium Chloride
NHS	Normal human serum
PAGE	Polyacrylamide gel electrophoresis
PC	Phosphocholine
PNA	Peanut agglutinin
SPR	Surface plasmon resonance
SD	Standard Deviation
SDS	Sodium Dodecyl sulphate
SNA	*Sambucus nigra* agglutinin
TB	Tuberculosis
TCA	Trichloro acetic acid
UEA	*Ulex europaeus* agglutinin
VL	Visceral leishmaniasis
WGA	Wheat germ agglutinin

Introduction

Human C-reactive protein (CRP) is a member of the pentraxin family of proteins and is an acute phase protein. Due to exposure of acute phase stimulus, the levels of CRP increases rapidly from <1 μg/ml to 1 mg/ml approximately within 24–48 h [1–3]. CRP is synthesized mainly from liver as well as non-hepatic tissues under certain circumstances [4, 5]. It is able to bind to exposed phosphocholine (PC) on the cell surface in a calcium-dependent manner [6]. However, a new ligand, Protein-A has also been demonstrated establishing the extended definition of human CRP [7]. Earlier we have reported that the glycosylated molecular variants of human CRP appeared in several pathological conditions [8] and interact with many biological macromolecules [9].

A detailed knowledge of the ligands identified by CRP is crucial for understanding of its role in host defence and homeostasis. CRP being a pattern recognition molecule can bind to varieties of ligands *viz.* chromatin and histone [10, 11] along with lymphocytes [12]. When bound to PC-containing substrates or polycations, CRP is known to activate the classical complement-cascade via C1q [13–15]. Although CRP able to bind with a variety of blood cells, it remains to be investigated whether CRP interact *in vivo* as a free serum protein, or when it is bound to cell surfaces [16].

The knowledge regarding potential pathways for *in vivo* clearance of human erythrocytes is inadequate [17, 18]. Here, we have selected two most widespread diseases of India *viz* tuberculosis (TB) and *visceral* leishmaniasis (VL). The present study elucidated the interaction of purified glycosylated molecular variants of CRP with diseased-erythrocytes. This binding of CRPs was through a few specific molecules on erythrocytes. Significant changes of membrane characteristics of erythrocytes resulted in CRP-induced complement-mediated hemolysis. This probably established the modulatory role of glycosylated CRPs in this process. To the best of our knowledge, our data provide evidence that glycosylated molecular variants of CRP activate complement-mediated hemolysis of erythrocytes and may account for the causative anemia, a common clinical manifestation in TB and VL.

Materials and methods

Patients and controls

Blood samples (n=85) from clinically confirmed and diagnosed individuals with TB (n=30) and VL (n=30) with no apparent co-infection and age-matched normal

healthy donors (n=25) of either sex were included in this study (Table 1). The TB patients were included based on the clinical findings, chest radiographs and presence of TB bacilli in sputum or tissue smears. Diagnosis of VL was established by microscopic demonstration of amastigotes in bone marrow or spleen aspirates performed at clinics, as per World Health Organization recommendation (website: http://www.who.int/tdr/research/progress/leish_prd/summary.htm). Individuals were devoid of any other red cell disorder and parasitic infections. With informed consent, blood samples were collected to obtain erythrocytes in sterile vacutainer containing anticoagulant Alsever's solution (114 mM citrate, 27 mM glucose, 72 mM NaCl, pH 6.1), centrifuged, washed, buffy coat removed and used within 2–4 h of collection. Fresh sera were obtained by clotting blood samples without anti-coagulant at 25–30°C. The Indian Council of Medical Research and the Institutional Human Ethical Committee approved this study.

Purification and characterization of human CRP

Serum samples showing elevated levels of CRP by latex agglutination (Rhelax-CRP kit, Tulip, India) were selected for purification. CRPs were separately purified from patients (n=12) with TB and VL and designated as CRP_{TB} and CRP_{VL} respectively [8, 19]. The serum amyloid-P (SAP) component was initially removed by passing the serum (5.0 ml) through an agarose bead column in the presence of Tris (50 mM Tris/HCl) buffered saline (150 mM NaCl, pH 7.5, TBS), with $CaCl_2$ (5.0 mM). Subsequently, SAP free serum was passed through a Sepharose—PC affinity column in TBS (20 mM Tris/HCl) and $CaCl_2$ (10 mM), pH 7.5. The bound proteins were eluted with EDTA (10 mM) containing $CaCl_2$ (1.0 mM). The eluted protein were dialyzed with TBS before adjusting the calcium concentration to 10 mM, and allowed to bind to a second Sepharose—PC affinity column. This column was washed with TBS containing $CaCl_2$ (10 mM). Pure CRP was eluted with PC (2.0 mM) in TBS, pH 7.5 containing $CaCl_2$ (0.50 mM). Finally, the eluted protein was dialyzed extensively against Hepes (20 mM) with saline containing EDTA (2.0 mM), followed by same buffer without EDTA. Purified CRPs were stored at -20°C without sodium azide and used within 2-weeks. The protein was estimated using the extinction coefficient, $E^{1cm}_{1\%}$ at 280 nm of 19.50 [20] and also by Lowry method [21]. Human CRP, till its discovery

Table 1 Clinical and laboratory features of the patients

Hematological parameters[a]	Patients (Range)		Normal (Range)
	TB (n=30)	VL (n=30)	(n=25)
Age, mean, years	30–45	25–40	20–40
Duration of illness (days)	30–60	60–90	–
Spleen size (cm) (below left lower costal margin)	3–4	7–11	Non palpable
Red blood cells count (millions/cubic millimetre)	2.0–4.2	1.5–3.5	4–6
White blood cells count (10^3/cmm)	12–13	10–11	4–11
Reticulocyte count (%)	0.2–1.0	0.6–1.2	0.2–2.0
Platelet count (10^3/μl)	200–300	100–400	150–450
Neutrophil (%)	35–50	35–48	50–70
Lymphocyte (%)	45–65	40–58	20–40
Hemoglobin (g/dl)	7 – 8	6.1–8.0	14–16
Hematocrit (%)	33–37	29–35	40–52
Mean Corpuscular volume (Feltolitre)	73–79	75–82	82–92
Mean Corpuscular Hemoglobin (Picogram)	21–26	20–27	26–32
Mean Corpuscular Hemoglobin Concentration (%)	29–32	25–30	31–35
Urea (mg/dl)	25–70	20–60	10–50
Creatinine (mg/dl)	0.7–2.0	0.8–1.7	0.7–1.5
Total Bilirubin (mg/dl)	0.25–9.0	0.3–0.9	0.25–1.0
Total protein (g/dl)	4.5–7.0	6.5–9.0	6.0–8.5
Albumin (g/dl)	2.9–5.2	3.0–5.0	3.2–5.5
Globulin (g/dl)	2.0–3.2	3.0–4.9	2.4–3.5
Erythrocyte Sedimentation Rate (mm/1st hr)	45–98	35–90	0–20

[a] Clinically confirmed blood samples from patient and age-matched normal individuals was collected in Alsever's solution and used within 2–4 h. Each clinical parameter was dictated by Clinicians and represented in a range value

was reported to be a non-glycosylated protein [22], but our laboratory for the first time, has demonstrated that human CRP is glycosylated in certain pathological conditions [8]. For comparison, we have used commercially available non-glycosylated CRP from Sigma, CRP_{Sigma}, purified from human plasma as internal control.

The purity of CRPs was checked by SDS-PAGE (10%) under reducing conditions [23]. Molecular masses of the subunits were detected by using the standard SDS-PAGE markers along with purified human IgG. CRPs were >99% pure based on reactivity with anti-human CRP in Western blotting [24] and no detectable band was observed with anti-human IgG antibodies. CRP_{TB} and CRP_{VL} were radiolabeled with $Na^{125}I$ (1.0 mCi) [25] with a specific activity ~2×10^6 cpm/μg protein. The ^{125}ICRPs were passed on a Sepharose-PC column, washed and subsequently radioactive CRPs were eluted using similar purification protocol. Approximately 99% of the total radioactivity was observed in bound protein as detected by TCA precipitation. Approximately >95% ^{125}ICRPs bound to Sepharose-PC in the presence of Ca^{+2}, indicated no loss of binding properties of the native protein. The purity of eluted ^{125}ICRPs was further checked by autoradiographs after SDS-PAGE analysis. ^{125}ICRPs were stored at 4°C and used within 2-weeks.

The degree of glycosylation and sialylation was detected using equal amounts of CRP (1.0 μg/spot) by a digoxigenin (DIG) enzyme-immunoassay using a DIG-glycan detection and differentiation kits according to manufacturer's instructions (Roche Molecular Biochemical). The developed spots were scanned and quantified in arbitrary units (Image Master Totallab Software, Amersham Pharmacia Biotech). The terminal sugars along with their specific-linkages were analyzed using several lectins, namely *Maackia amurensis* agglutinin (MAA), *Galanthus nivalis* agglutinin (GNA), *Sambucus nigra* agglutinin (SNA), peanut agglutinin (PNA) and *Datura stramonium* agglutinin (DSA). In parallel, ^{125}ICRPs were incubated separately with Sepharose-bound lectins (20 μl) of different sugar-linkage and specificity (Table 2), *e.g.* Concanavalin A (Con A), *Ulex europaeus* agglutinin (UEA), Wheat germ agglutinin (WGA), *Dolichos biflorus* agglutinin (DBA), MAA and SNA, overnight at 4°C. After extensive washing to remove unbound radioactivity, bound radiolabeled CRPs were monitored in a Gamma-counter. All experiments were performed twice in triplicate.

The presence of neutral sugars in CRPs was detected by GLC as their alditol acetates as described earlier [8, 26]. CRPs (100 μg) were hydrolysed with trifluroacetic acid at 120°C for 90 min to liberate monosaccharides. This was followed by reduction with sodium borohydride. The generated alditols were acetylated with acetic anhydride and distilled pyridine at 22–25°C for 16 h. A GLC instrument using a Hewlett-Packard 6890 plus gas chromatograph equipped with a flame ionization detector was used for analysis. Each constituent sugars were identified from the retention time of authentic sugars. A Hewlett-Packard 3380A chemstation was used for the detection and quantitation of the peaks. A fused-silica capillary column HP-5 (30 m, 0.32 mm, 0.25 μm) along with carrier gas nitrogen was used for resolution with a temperature program of 150°C (5 min), 2°C (1 min) and 200°C(10 min) at split less mode [27].

Glycosidically bound sialic acids were released by hydrolysing CRPs (100 μg/500 μl) at 80°C for 1 h with trifluoroacetic acid (0.05 M). The hydrolysate was evaporated and co-distilled with water (0.5 ml×3) to remove all traces of acid [8]. The sample was dried under vacuum over P_2O_5 for 4 h. The hydrolyzed sample was dissolved and analyzed by Ion Chromatography System (ICS3000, Dionex Corporation, USA) using a PA10 Carbopack column (2× 250 mm) at 32°C isothermal conditions. Chromeleon software (v 6.8) was used for detection and estimation of peaks. For resolution, aqueous solution A (200 mM NaOH) and B (1 M NaOAc) was used with an initial concentration of A (93%) and B (7%) for 10 min and subsequently, A (70%) and B (30%) for 4 min showing a linear gradient. The *N*-acetyl neuraminic acid present in hydrolysed CRP (0.8335 μg/25 μl) was identified by direct comparison with standard solution of sialic acid (Sigma, St. Louis, USA).

CRPs (50 μg) were also hydrolysed with an equal volume of propionic acid (4 M) for 4 h at 80°C, cooled on ice for 10 min. Sialic acids were purified through Dowex 50 W x 8 (100–200 mesh) cation and Dowex 2×8 (200–400 mesh) anion exchange columns [28]. Purified sialic acids were derivatized with DMB and directly analyzed by MALDI-TOF-MS (Applied Biosystem, USA). The samples were prepared by dried-droplet procedure using 2, 5-dihydroxybenzoic acid (10 μg/μl, DHB) using ethanol (60%) as matrix. All mass spectra were recorded in the positive ion mode using the reflector. The ion acceleration potential and the potential in the reflector were 10.5 kV and 9.7 kV respectively. The acquired spectra were the average of 1000 laser shots.

To reconfirm the presence of sugars in the induced CRPs, they were deglycosylated. Fixed amounts of CRP_{TB}, CRP_{VL} and CRP_{Sigma} were initially incubated overnight with *Arthrobacter ureafaciens* neuraminidase (specific activity, 0.5 mU) in denaturation buffer at pH 8.6 at 37°C and then heated at 100°C for 3 min as described earlier [8]. The reaction mixture was centrifuged and *N*-glycosidase F was added and incubated overnight at 37°C in presence of CHAPS at pH 7.2. Additionally, neuraminidase treated samples were incubated overnight with the *O*-glycosidase (1-2 mU) in potassium phosphate buffer containing EDTA, Triton X and SDS, pH 7.3 at 37°C. Deglycosylated CRPs were passed on a Sepharose-PC column to remove enzymes present in the reaction mixture and further analyzed by SDS-PAGE (10%). Analytical isoelectric focusing [29] of glycosylated and deglycosylated CRPs (1.5 μg) from TB (*n*=

Table 2 Status and glycosylation profile of purified CRP_{TB} and CRP_{VL}

Parameters for molecular characterization of CRPs	Lectin (sugar and linkage specificity) and sugar	CRP_{TB} (n=6)	CRP_{VL} (n=6)
CRP in crude serum[a]		+++	+++
Concentration of purified CRPs (μg/ml) [b]		57–75	55–98
Fold increase[c]		114–150	110–196
Sugar[d]		8,989±283	10,921±1194
Sialic acid[e]		10,200±250	9,000±200
Binding as reflected by densitometric scores[f]	MAA [Neu 5Ac α (2–3) Gal/GalNAc]	7000±325	9240±125
	GNA [Man α(1–3),(1–6) and (1–2)Man]	6400±225	6325±188
	SNA [Neu5Ac α (2–6) Gal/GalNAc]	–	–
	PNA [Galβ (1–3) GalNAc]	–	–
	DSA [Galβ (1–4) GlcNAc]	–	–
Lectin binding (%)[g]	ConA (α-Man, α-Glc)	12.18	8.2
	MAA	11.7	6.2
	SNA	2	0.87
	WGA (GlcNAc, Neu5Ac)	6.03	2.5
	UEA (α-L-Fuc)	7.3	4.03
	DBA (α-GalNAc)	3.037	1.7
Intensity (%)[h]	Neu5Ac	65%	42%

[a] Fresh sera, obtained by clotting clinical blood samples at room temperature, showing strong visible agglutination (+++) by latex Rhelax-CRP kit (Tulip, India) were selected for CRP purification

[b] The protein concentration was estimated using the extinction coefficient, $E^{1cm}_{1\%}$ at 280 nm of 19.50

[c] Fold increase of purified CRPs was calculated considering 0.5 μg/ml as normal level

[d, e, f] The intensities of the developed spots (Fig. 1b,c) were quantified and reported as mean ± SD of densitometric score in arbitrary units from two independent experiments ($p<0.001$)

[g] [125] ICRPs were incubated with Sepharose-bound lectins (20 μl) and binding (%) was determined as described in Methods. All experiments were performed twice in triplicate, and a representative profile was reported here

[h] The Intensity (%) of Neu5Ac with an m/z of 448.7 was derived from MALDI-TOF analysis

3) and VL (n=3) patients were carried out in capillary tubes on ampholine polyacrylamide gel (4%), pH range, 3.5 – 10.0 using Mini-PROTEAN II tube cell apparatus (Biorad) at a constant voltage of 400 V for 6 h. The focused tube gels were fixed, washed and stained with silver nitrate [8]. The isoelectric point (pI) of the individual protein was determined as a function of their migration from the cathode using standard proteins (Sigma).

Binding of erythrocytes with disease-associated CRPs

Different molecular variants of glycosylated, deglycosylated and commercial non-glycosylated CRPs (CRP_{Sigma}) were incubated separately in TBS (2.0 mM $CaCl_2$, 1.0 mM PC, pH 7.5) for 1 h on ice and designated as CRP-PC-Ca^{+2} complex. This complex was used subsequently in all the following experiments.

i. Flow-cytometry

The FITC was conjugated to CRP [30]. The binding of erythrocytes ($1x10^9$) from TB (E_{TB}), VL (E_{VL}) and normal individuals (E_N) with respective FITC-CRP_{TB} or FITC-CRP_{VL} (0.05 - 1.0 μg) was evaluated by flow-cytometry (CELLQUESTPRO software, Becton Dickinson FACSCalibur). Glycosylated and deglycosylated FITC-CRP_{TB}-PC-Ca^{+2} or FITC-CRP_{VL}-PC-Ca^{+2} complex were incubated with E_{TB} and E_{VL} for 1 h on ice, washed and fixed with 1% paraformaldehyde (Sigma). Specific binding was determined by pre-incubation of 50-fold excess of unlabeled respective CRP to CRP-PC-Ca^{+2} complex. Under identical conditions, the experiments were carried out using E_N with FITC-CRP_{TB}, FITC-CRP_{VL} and FITC-CRP_{Sigma}. In parallel, cross-binding studies were carried out by reacting E_{TB} with FITC-CRP_{VL} or E_{VL} with FITC-CRP_{TB}. Bound CRP (if any) on the erythrocytes was determined by incubating cells with polyclonal murine anti-human CRP (1: 100) followed by FITC-anti-murine IgG (1:500). Only cells or E_N, FITC-BSA served as different sets of controls.

ii. Scatchard analysis

Erythrocytes were suspended with TBS-Ca^{+2}-1.0% BSA for 1 h on ice. Increasing doses of ^{125}ICRP_{TB}-PC-Ca^{+2} or

$^{125}ICRP_{VL}$-PC-Ca^{+2} complex were incubated separately with E_{TB} or E_{VL} or E_N (1×10^9/30 µl, n=18) for 1 h on ice. Following washing with TBS-Ca^{+2}-BSA, cell-bound radioactivity was quantified in a Gamma-Counter (Electronic Corporation of India). Specific binding was determined from the difference between total binding and the binding in presence of 50-fold excess of unlabeled CRP. Scatchard plots of the binding data was used to calculate the association constant (K_a) [31] and the number of receptor-sites/cell in both diseased and normal erythrocytes. Measurements were done twice in triplicates.

iii. ELISA

Erythrocyte membranes from patients and healthy normal individuals were prepared by re-suspending erythrocytes in ice-cold buffer containing digitonin (1.0 mg/ml) for 20 min at 0°C [32, 33]. The membrane proteins were dissolved in equal volume of extraction buffer (20 mM Tris-HCl, pH 7.5; 1.0%Triton X-100; 0.1% SDS; 200 mM NaCl) for 1 h at 0°C and centrifuged. The supernatant containing only membrane proteins was quantified [21]. Membrane proteins from TB and VL patients along with normal were immobilized (2.0 µg/well/100 µl) separately on microtitre plates (Nunc, USA), overnight at 4°C. The wells were washed with TBS-Tween (0.01%, TBS-T), blocked (TBS-2% BSA) and incubated overnight at 4°C with varying concentrations of CRP_{TB}-PC-Ca^{+2} and/or CRP_{VL}-PC-Ca^{+2} complex separately. Washed wells were incubated with polyclonal murine anti-human CRP antibodies (1:2000). The bound complex was detected by peroxidase-goat anti-murine IgG (1:8000, Cappel) using azino-bis-thiosulphonic acid (ABTS) as substrate and quantitated by an ELISA Reader (Thermo Electron Corporation) at 405 nm. The control wells were devoid of either membrane protein or CRP. In parallel, immobilized normal erythrocyte membrane were allowed to bind with CRP_{Sigma}-PC-Ca^{+2} complex and processed similarly. To determine the bound CRP on the erythrocytes, membrane protein in the well was allowed to react with polyclonal murine anti-human CRP followed by HRP-conjugated anti-murine IgG.

iv. Surface plasmon resonance (SPR)

The interaction between CRP and erythrocyte membrane proteins from patient and normal donors was performed by SPR experiment (Biacore 3000,Biacore). Each flow cells of a CM5 sensor chip were activated at 25°C at a flow rate of 5 µl/min by passing a mixture (20 µl) of 1-ethyl-3-(3-dimethylaminopropyl) carbodiimide (0.20 M) and *N*-hydroxy-sulfosuccinimide (0.05 M), after which CRP_{TB} or CRP_{VL} was injected. Physiological concentration of CRPs (10 µg/ml) in sodium acetate (10 mM, pH 4.5) was immobilized onto the carboxymethylated dextran surface of a CM5 sensor chip using the amine coupling chemistry. Ethanolamine (1 M, 20 µl, pH 8.5) was used to block unreacted groups. The flow buffer was HEPES (10 mM), NaCl (150 mM) pH 7.5 along with $CaCl_2$ (2 mM), PC (1.0 mM) and Tween-20 (0.001%). As negative control, activated and blocked flow cell were used as blank sensograms for substraction of the bulk refractive index background. Samples were first injected over the control chip and then over immobilized CRP. Erythrocyte membrane protein (10–50 µg/ml) at a flow rate of 30 µl/min was passed. Association and dissociation times were 5 and 3 min, respectively. Regeneration was achieved by injecting NaCl (2 M, 30 µl). Sensograms were analyzed with the Biaevaluation software (v 4.1). Resonance responses (RU) (arbitrary units) were plotted against the varying concentrations of erythrocyte membrane protein for both the patient and normal samples.

v. Western blot anlysis

Erythrocyte membrane protein (50 µg/ lane) from individual TB (n=12) or VL (n=12) patients or normal (n=8) was electrophoresed separately on reducing SDS-PAGE (7.5%). The separated proteins were transblotted on a nitrocellulose paper, blocked (TBS-2%BSA) and incubated separately with CRP_{TB}-PC-Ca^{+2} and/or CRP_{VL}-PC-Ca^{+2} (5.0 µg) in TBS-BSA for overnight at 4°C. Membranes were washed with TBS-Ca^{+2}-T, incubated with polyclonal murine anti-human CRP (1:500) for overnight at 4°C and followed by HRP-conjugated rabbit anti-murine IgG (1:1000) in TBS-BSA, washed and visualized by 3, 3-diaminobenzidine (DAB). Similar experiments were carried out with normal erythrocyte membrane proteins and CRP_{Sigma}-PC-Ca^{+2} complex. Pre-stained markers were used as standard.

In an attempt to purify bound CRP on erythrocyte, membrane proteins (400 mg) were passed through first and second Sepharose-PC affinity-column as described before. PC eluted material was analyzed by SDS-PAGE.

vi. Immunoprecipitation experiments

Erythrocyte membrane proteins (50 µg/25 µl) from TB or VL or normal were incubated separately with CRP_{TB}-PC-Ca^{+2} or CRP_{VL}-PC-Ca^{+2} and/or CRP_{Sigma}-PC-Ca^{+2} (5.0 µg) in TBS-BSA for overnight at 4°C, and incubated with polyclonal rabbit anti-human CRP (1:100/100 µl) for overnight (4°C). This was followed by incubation with Protein A-Sepharose 4B (5 µl, 6 mg/ml, Sigma) for overnight at 4°C. The Sepharose-bound protein complexes were washed with cold TBS. The protein samples were boiled with Laemmli sample buffer (4x) for 10 min and centrifuged. The supernatant was further incubated overnight with Protein A-Sepharose 4B (5 µl) and centrifuged. Supernatant was boiled again with Laemmli sample buffer (4x) and loaded on each lane. The proteins were separated on SDS-PAGE

(7.5%) followed by electrophoretic transfer to nitrocellulose paper. The blots were incubated with CRP_{TB}-PC-Ca^{+2} or CRP_{VL}-PC-Ca^{+2} and/or CRP_{Sigma}-PC-Ca^{+2} separately. Subsequently the blots were probed with polyclonal murine anti-human CRP (1:500) and processed as described above.

Detection of membrane characteristics of erythrocytes

i. Osmotic fragility

E_{TB}, E_{VL} and E_N (1×10^9) were incubated with respective CRP_{TB}-PC-Ca^{+2} or CRP_{VL}-PC-Ca^{+2} complex (5.0 μg) for 1 h at 37°C, washed with TBS-Ca^{+2} and further exposed to different NaCl concentrations (0.3–0.9%) for 1 h at 37°C [34]. Only cells in TBS-Ca^{+2} served as control. Lysis of erythrocytes in distilled water was taken as 100%. The hemolysis (%) of erythrocyte (osmotic fragility) was measured before and after binding with CRP_{TB} or CRP_{VL} as follows:

$$Hemolysis\,(\%) = (OD_{412}\,nm\ at\ particular\ saline\ concentration / OD_{412}\,nm\ with\ distilled\ water) \times 100.$$

ii. Membrane fluidity

Ghost membrane (0.2 mg/ml) from erythrocytes of TB, VL and normal was incubated with respective CRP_{TB}-PC-Ca^{+2} or CRP_{VL}-PC-Ca^{+2} complex (5.0 μg) for 1 h at 0°C. A fluorescent probe, 1,6-diphenyl-1, 3, 5-hexatriene (DPH) was used for determination of fluidity of erythrocyte ghost membrane by steady state fluorescent polarization [34]. The probe after binding with membrane when illuminated by polarized light emitted a fluorescence signal, which reflected the motion in the membrane lipid environment. DPH was excited by vertically polarized light at 340 nm and its emission intensities were detected at 420 nm through a polarizer oriented parallel (I_v) and perpendicular (I_h) to the direction of polarization of excitation beam. The fluorescence was measured using a fluorescence spectrophotometer (Hitachi F 4050, Hitachi Ltd, Japan). Fluorescence anisotropy (r_s) is inversely related to membrane fluidity. This was calculated according to the equation:

$$r_s = I_v - I_h / I_v + 2I_h$$

iii. Hydrophobicity

Washed E_{TB}, E_{VL} and E_N (1×10^9) were separately incubated initially for 1 h at 0°C with respective CRP_{TB}-PC-Ca^{+2} or CRP_{VL}-PC-Ca^{+2} complex (5.0 μg), washed with TBS and further incubated with 8-anilino-1-napthalenesulfonic acid (ANS, 5.0 μl, 1.0 mM) at 37°C. Fluorescence spectra were recorded (400–700 nm). Excitation wavelength was 365 nm and the band passes of excitation and emission were of 5 nm [34].

Complement-mediated hemolysis after erythrocyte-CRP binding

Washed E_{TB}, E_{VL} and E_N (1×10^9, n=15) were initially incubated with respective CRP_{TB}-PC-Ca^{+2} or CRP_{VL}-PC-Ca^{+2} complex (0.10–10 μg/ml), for 1 h at 0°C, washed with ice-cold gelatin-veronal-buffered (GVB) saline containing Ca^{+2} (0.15 mM) and gelatin (0.1%). Activation of complement pathway was assessed by further incubating these CRP-bound erythrocytes for 1 h at 37°C in the presence of either normal human serum (NHS, diluted 1:50 in GVB buffer, 100 μl) or patients' serum or CRP-depleted patient's serum, which served as different sources of complement [35]. The reaction was diluted with GVB buffer (1.0 ml, 4°C), centrifuged and the extent of hemolysis was recorded in the supernatant at 412 nm, as described above. Cells in distilled water show 100% hemolysis. Deglycosylated CRPs (10 μg/ml), decomplemented NHS and guinea pig serum, 10 mM EDTA and anti-CRP antibodies were used as different controls. Experiments were done in triplicates and reported as mean ± SD.

Statistical analysis

Statistical analyses were performed using the Graph-Pad Prism statistics software (Graph-Pad Software Inc., USA). Student's t-tests were used and p values <0.05 were considered as statistically significant at 95% confidence interval.

Results

Molecular characterization of purified glycosylated CRPs

CRPs were purified separately from individual patients with TB and VL (Fig. 1a, Table 1). The amount of CRP in serum of these patients was in the range of 55–98 μg/ml indicating 110–196-fold increase above the normal level (0.5 μg/ml). Only two calcium-binding proteins were eluted from first PC column (lane 3) from the major proteins present in SAP free sample (lane 2). Single band after PC elution from second PC column was taken as pure CRP with differences in their subunit molecular weight indicating the presence of molecular variants in CRP_{TB} (lane 4, 29 kDa) and CRP_{VL}

(lane 5, 28 kDa) samples. CRP_{Sigma} showed a single band with a subunit molecular weight of 23 kDa (lane 6). The subunit molecular weight for disease-associated CRPs was always higher than CRP_{Sigma}, which coincided with that of the reported molecular weight (23 kDa) of normal CRP [36]. Autoradiographs of $^{125}ICRP_{TB}$ (lane 7) and $^{125}ICRP_{VL}$ (not shown in figure) showed single band in SDS-PAGE. CRP_{TB} (lane 8) and CRP_{VL} (lane 9) showed single band with anti-human CRP antibodies in Western blotting confirming their homogeneity as also observed earlier [8]. Although standard human IgG showed strong bands with polyclonal anti-human IgG (lane 10), under identical condition, purified CRPs showed no detectable band in Western blotting confirming the absence of human IgG (lane 11).

As reported earlier [8], purified CRP_{TB} and CRP_{VL} from these group of patients also demonstrated the presence of differential glycosylation (i) and sialylation (ii) as evident from the intensities of spots by densitometric scanning (Fig. 1b, Table 2). CRP_{Sigma} showed no reactivity indicating the absence of glycosylation and sialylation. Wide variations in the carbohydrate moieties of CRP_{TB} and CRP_{VL} were demonstrated by differential binding towards the different lectins tested as shown in Table 2 [8]. Both CRP_{VL} and CRP_{TB} showed strong binding with MAA and negligible binding with SNA suggesting predominance of α(2–3)-linked sialic acids as shown in Fig. 1c [8, 9]. Equal binding of GNA with CRP_{TB} and CRP_{VL} revealed the presence of terminal Man α(1–3), (1–6) and (1–2) mannose linkages. In contrast, no reactivity was observed with PNA and DSA indicating absence of both Gal β(1–3) GalNAc and Gal β(1–4)GlcNAc motif (Fig. 1c, Table 2). The binding of $^{125}ICRPs$ with Con A and MAA corroborated the presence of mannose, glucose and α(2–3)-linked sialic acids. MAA and WGA binding revealed differential presence of Neu5Ac in these two CRPs. UEA revealed the presence of α-L-Fuc. However, low DBA binding may be due to the presence of less α-GalNAc (Table 2).

The differential glycosylation of these two CRPs was further investigated by GLC. The chromatogram peaks of CRP_{TB} [8] and CRP_{VL} revealed striking differences between the presence of three hexoses, namely mannose, glucose and galactose. GLC analysis does not revealed the presence of other hexoses. The amounts (%) of three hexoses in a representative CRP_{VL} sample are 63.54%, 15.15% and 13.59% respectively (Fig. 1d). The retention time (RT) of mannose, glucose and galactose are 13.85, 15.21 and 16.87 min respectively. As the molecular weights of all these hexoses are same, their amount (%) may be considered to be proportional to their molar ratios. No detectable peak for different hexoses in GLC profile was obtained for CRP_{Sigma} suggesting absence of glycosylation.

The sialic acid content of CRP_{TB} and CRP_{VL} was also determined by Ion Chromatography. A representative profile of the analysis of CRP_{TB} is presented in Fig. 1e. The Ion Chromatography peaks revealed the presence of sialic acid as compared with the standard sialic acid. Nearly 7% sialic acid was observed in CRP_{TB}. No detectable peak was observed in CRP_{Sigma} suggesting absence of sialic acid. The presence of sialic acids on CRPs was investigated by MALDI-TOF-MS following the release of sialic acid and labelling with DMB. A peak coincided with an m/z of 448.7 reflected the presence of Neu5Ac.

Fig. 1 Purification and characterization of glycosylated CRP from serum of patients with TB and VL. **a** *Electrophoretic analysis*. Equal amounts of serially purified fractions from serum of a representative patient with tuberculosis (TB) were electrophoretically analyzed on a SDS-PAGE (10%). Lane 1, crude serum; lane 2, unbound fraction from agarose column; lane 3, EDTA eluates from 1st PC column; lane 4, PC eluates from 2nd PC column (CRP_{TB}); lane 5, CRP from a representative patient with VL (CRP_{VL}) was purified similarly and analyzed by SDS-PAGE. Single band of commercially purified CRP_{Sigma} are shown in lane 6. Lane 7 is autoradiograph of ^{125}I CRP_{TB}. Western blotting of equal amount (14 μg) of PC eluted fraction from a patient with TB (lane 8) and a patient with VL (lane 9) probed with murine anti-human CRP and detected by HRP-anti-murine IgG. For comparison, Western blotting of standard human IgG (lane 10) and CRP_{TB} (lane 11) with HRP-anti-human IgG are shown. **b** *Detection of glycosylation and sialylation of CRPs*. Profile of glycosylation (▣, i) and sialylation (□, ii) as analyzed by DIG-enzyme-immunoassays were carried out using purified CRPs (1.0 μg/spot) and CRP_{Sigma}. CRPs were blotted on nitrocellulose strips and processed as described in Materials and Methods. Densitometric scanning scores of CRP_{TB} and CRP_{VL} along with positive (+) and negative (-) controls is shown in bar graph. Results are reported as mean ± SD of densitometric score in arbitrary units from three independent experiments ($p<0.001$). **c** *Differential glycosylation pattern in CRPs*. CRPs purified from TB and VL patients were analyzed for detection and linkage specificity of carbohydrate chains using MAA, GNA, SNA, PNA and DSA lectins by DIG glycan differentiation kit as described in Materials and Methods. Carboxipeptidase Y (GNA+), fetuin (MAA, SNA and DSA+) and asialofetuin (PNA and DSA+) were used as positive controls ('+'). **d–e** *Analysis of carbohydrate composition by GLC and Ion Chromatography*. **d** A representative profile for the presence of three hexoses in purified CRP (100 μg) from a VL patient as analyzed by GLC. The analysis was carried out as described in Materials and Methods. Response (pico ampere, pA) was plotted against time (min). The individual peaks represented in relative percent area revealed the presence of mannose, glucose and galactose. **e** *Analysis of sialic acid by Ion Chromatography*. A representative profile for the presence of sialic acid in CRP_{TB} (100 μg) is shown. The peak was compared with that of standard sialic acids. Response (in nano coulomb, nC) was plotted against time (min). **f** *SDS-PAGE before and after treatment with N-glycosidase F*. A representative profile of glycosylated CRPs purified from two individuals suffering from TB (29 kDa) and VL (28 kDa) as analyzed by SDS-PAGE (10%) is shown. Each sample was digested separately with *N*-glycosidase F at 37°C overnight and analyzed similarly. Non glycosylated CRP_{Sigma} processed similarly. A 23 kDa band was observed both before and after enzyme treatment. Protein bands were detected by Coomassie staining. **g** *IEF of purified CRP_{TB} and CRP_{VL}*. CRP (1.5 μg) was applied to ampholine polyacrylamide tube gel (4%) in a pH gradient (3.5–10.0) and stained with silver nitrate. A representative profile of glycosylated CRP_{TB} (pI 9.0), CRP_{VL} (pI 8.5) before and after *N*-glycosidase F treatment are shown respectively

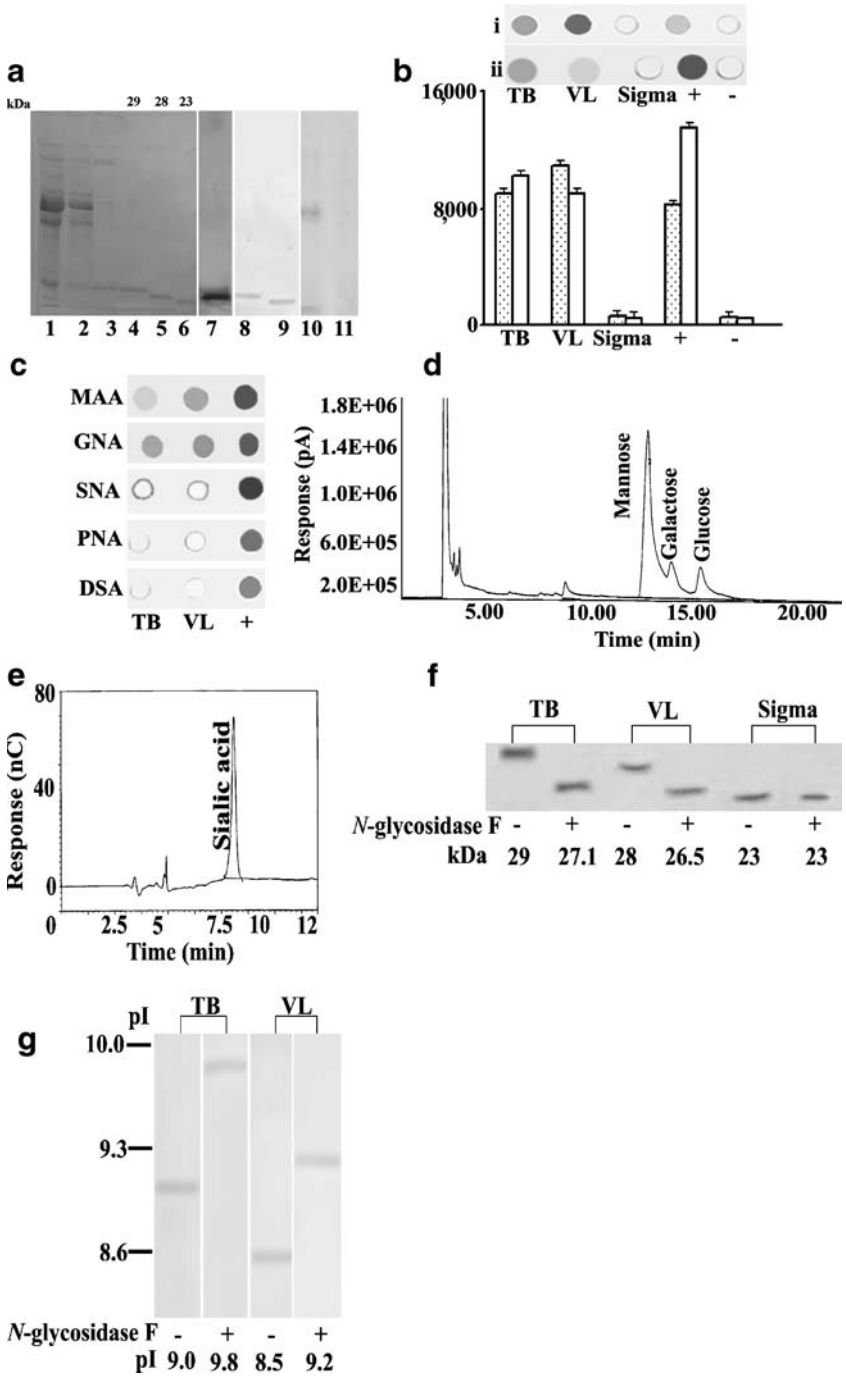

As demonstrated earlier [8] a decrease in the molecular mass of 1.89 kDa and 1.50 kDa respectively was observed after *N*-glycosidase F-digestion of CRP_{TB} (29 kDa) and CRP_{VL} (28 kDa) in SDS-PAGE suggesting glycosylation possibly through *N*-linkages (Fig. 1f). No such decrease in molecular mass was observed following *O*-glycosidase digestion of the same samples, suggesting absence of glycosylation through *O*-linkages. No changes in the electrophoretic mobility was observed following enzyme treatment of CRP_{Sigma}, once again confirmed that it is non-glycosylated (23 kDa).

A representative IEF gel profile [8] of CRP_{TB} and CRP_{VL} showed single band, corresponding distinct differences in their pI values are 9.0 and 8.5 respectively (Fig. 1g). It reconfirmed the purity and existence of a single molecular variant. After desialylation followed by deglycosylation, the pI values of CRP_{TB} and CRP_{VL} increased to 9.8 and 9.2 respectively. Taken together, these

observations suggested wide variations in glycosylation pattern induced in these two molecular variants of CRP (Fig. 1, Table 2) as corroborated by some of our earlier findings [7–9].

Binding of FITC-CRP with respective erythrocytes

The binding of FITC-CRP_{TB} and FITC-CRP_{VL} with corresponding erythrocytes (n=15) increased from 5% to >80 % with increasing concentrations of CRPs and it was saturated at nearly 1.0 μg. In contrast, the binding of FITC-CRP_{TB} and FITC-CRP_{VL} with E_N (n=8, p<0.001) was low (Fig. 2a). At 1.0 μg concentration, significant reduction in binding with FITC-CRP_{TB} (3.21±0.27-fold) and FITC-CRP_{VL} (2.61±0.21-fold) was observed with E_N as compared to patient erythrocytes. The presence of Ca^{+2} and PC facilitated the erythrocyte-CRP binding. The absence of PC or Ca^{+2} or both showed no significant binding (Fig. 2b). In presence of 50-fold excess unlabeled respective CRPs showed 4.2±0.5-fold and 6.0±0.2-fold reduced binding thus confirming the specificity of interaction between FITC-CRP_{TB} and FITC-CRP_{VL} towards respective erythrocytes (Fig. 2b).

As contrary to glycosylated CRP_{VL}, the binding of deglycosylated FITC-CRP_{VL} (1.0 μg) with E_{VL} was drastically reduced from 84±3% to 12±3% (p<0.001 Fig. 2b). Similarly, deglycosylated FITC-CRP_{TB} (1.0 μg) showed 5.93-fold reduced binding compared to glycosylated CRP_{TB}, % binding being 89±5 % vs. 15±2% (Fig. 2b). Deglycosylated CRPs also showed negligible binding with E_N, being 5 ±2% respectively. The binding of FITC-CRP_{Sigma} (1.0 μg) with E_N was nearly 3±1% (not shown in figure).

In parallel, cross-binding studies between E_{TB} with FITC-CRP_{VL} or E_{VL} with FITC-CRP_{TB} showed only 5±3% binding indicating that some common molecules are present both on patient or normal erythrocytes that reacted with CRPs.

To explore the presence of any CRP already bound on erythrocytes, cells were allowed to bind with anti-human CRP antibodies. Only 4±2% binding indicated that erythrocytes were possibly shielded with some CRP present in the serum *in vivo*. Cell only or FITC-BSA gives no binding suggesting the binding was specific for CRP.

Increased CRP-binding molecules on patients' erythrocyte after binding with CRP

Scatchard analysis revealed increased number of receptors on E_{TB} ($1.9\pm0.7\times10^7/E_{TB}$, Fig. 3a, inset) following binding with CRP_{TB}. In parallel, experiments were repeated using CRP_{VL} and the number of receptors on E_{VL} was found to be $1.7\pm0.5\times10^6/E_{VL}$ (Fig. 3b, inset). The specific nature of binding was evaluated by adding excess unlabeled CRP, the apparent K_a of $^{125}ICRP_{TB}$ with E_{TB} and $^{125}ICRP_{VL}$ with E_{VL} in presence of PC and Ca^{+2} being $2.30\pm0.55\times10^5\,M^{-1}$ (Fig. 3a) and $1.30\pm0.65\times10^4\,M^{-1}$ (Fig. 3b) respectively.

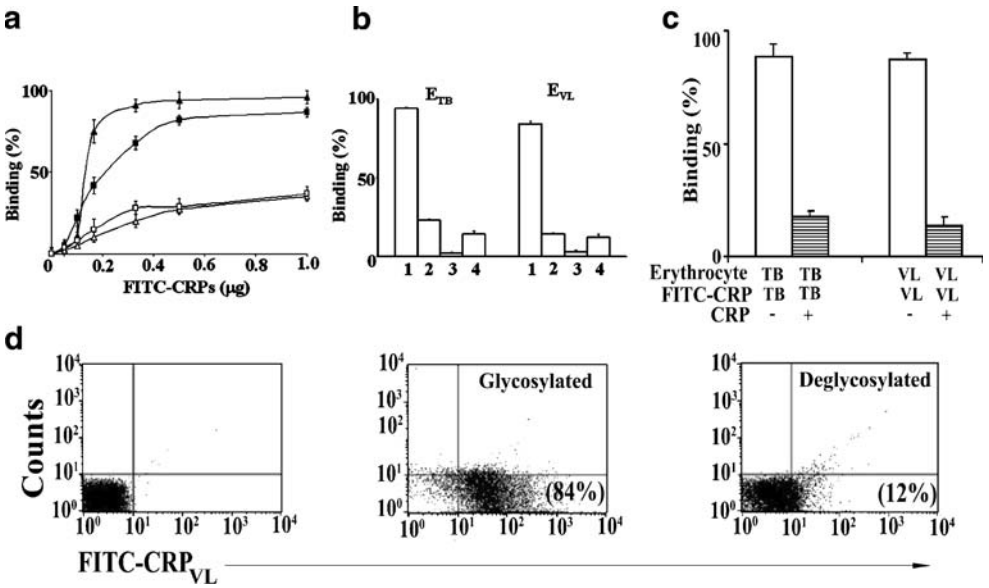

Fig. 2 Comparative analysis of binding of CRP_{TB} and CRP_{VL} with respective erythrocytes by FACS analysis. **a** *Dose-dependent binding of CRP with erythrocytes*. A fixed number of erythrocytes from TB (-▲-) and VL (-■-) were incubated with increasing concentration of respective FITC-CRP_{TB} and FITC-CRP_{VL} (0.05 – 1.0 μg) as described in Materials and Methods. The binding of normal erythrocytes with FITC-CRP_{TB} (-△-) and FITC-CRP_{VL} (-□-) are shown. **b** *Specificity of binding of CRP with erythrocytes*. Binding of erythrocytes from TB (E_{TB}) and VL (E_{VL}) with respective FITC-CRP_{TB} and FITC-CRP_{VL} (1.0 μg) in presence of both PC and Ca^{+2} (1), in presence of unconjugated CRP (2), absence of both PC and Ca^{+2} (3) and binding with respective deglycosylated FITC-CRPs (4)

In contrast, K_a for the interaction of E_N (n=8) with $^{125}ICRP_{TB}$ (Fig. 3c) and $^{125}ICRP_{VL}$ (Fig. 3d), are 4.23±0.03×$10^4 M^{-1}$ and 3.84±0.02×$10^4 M^{-1}$ respectively, corresponding CRP-receptors/E_N are 8.20±0.45×10^3/E_N (Fig. 3c, inset) and 5.1±0.20×10^3/E_N (Fig. 3d, inset) respectively.

Increased binding of CRPs with patient erythrocytes as analyzed by SPR

CRPs with approximately 2000 RU were immobilized on the CM5 chip. Representative sensograms of the association and dissociation phases of binding were recorded. The RU value of E_{TB}-CRP_{TB} and E_{VL}-CRP_{VL} binding significantly increased in concentration-dependant manner in the range of 10–50 μg/ml of respective membrane proteins (Fig. 4a,c). In contrast, E_N -CRP_{TB} and E_N-CRP_{VL} binding showed ~3–4-fold weaker resonance response in the same concentration gradient (Fig. 4b,d).

Increased binding of CRPs with membrane proteins from patients' erythrocytes

A dose-dependent binding of CRP_{TB} and CRP_{VL} with respective erythrocytes membrane proteins from TB (n=5) and VL (n=5) patients was observed (Fig. 4e). Both CRP_{TB} and CRP_{VL} (1.0 μg) showed strong binding; absorbance being 0.76±0.02 and 0.78±0.01 with E_{TB} and E_{VL} respectively. In contrast, 3.19±0.223 and 2.55±0.09-fold reduced binding of CRP_{TB} and CRP_{VL} was observed with E_N (n=8, p<0.001). The binding of CRP_{Sigma} with E_N (p<0.001) was negligible, absorbance being 0.08±0.04, thus signifying the disease-associated interaction.

The binding of E_{TB} and E_{VL} membrane proteins with anti-human CRP antibodies showed very low binding, absorbance being 0.10±0.03 and 0.09±0.01 respectively indicating that low amount of CRP possibly remained bound with erythrocytes, *in vivo*.

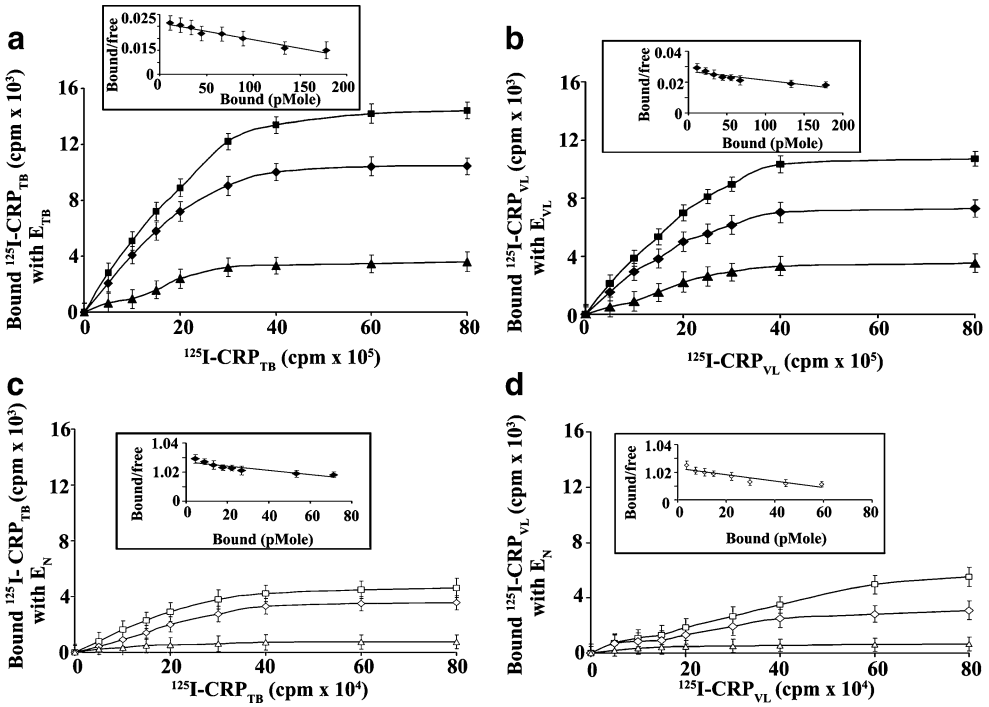

Fig. 3 Scatchard analysis of binding of $^{125}ICRPs$ with erythrocyte (E). **a** A fixed number of erythrocytes (1×10^9) from a TB patient (E_{TB}) were incubated with increasing amounts of $^{125}ICRP_{TB}$. For evaluating the specific nature of binding, a 50-fold excess of unlabeled CRP_{TB} was added. The bound and unbound CRP was separated at 4°C and the bound radioactivity was determined as described in Materials and Methods and plotted against added $^{125}ICRP_{TB}$. Specific binding (-◆-) was calculated by the difference between total binding (-■-) and binding in presence of excess unlabeled CRP_{TB} (-▲-). Results are expressed as mean ± SD of data from triplicate experiments (p<0.0001). Inset: Scatchard plot of the binding of $^{125}ICRP_{TB}$ to E_{TB} in which bound/free was plotted against the various amounts of bound CRP. **b** A fixed number of erythrocytes from a VL patient (E_{VL}) were similarly incubated with increasing amounts of $^{125}ICRP_{VL}$ as described in Fig. 3a. Specific binding (-◆-) was calculated by the difference between total binding (-■-) and binding in presence of unlabeled CRP_{VL} (-▲-). Inset: Scatchard plot of the binding of $^{125}ICRP_{VL}$ to E_{VL}. **c–d** Binding of $^{125}ICRP_{TB}$ (Fig. 3c) and $^{125}ICRP_{VL}$ (Fig. 3d) with erythrocytes from normal (E_N) were similarly processed. Specific binding (-◇-) was determined by the difference between total binding (-□-) and binding in presence of unlabeled CRP (-△-). Inset: Scatchard plots of the binding of $^{125}ICRP_{TB}$ (Fig. 3c) and $^{125}ICRP_{VL}$ (Fig. 3d) to E_N

Disease-associated CRP-binding molecules on erythrocyte membrane

To pinpoint the molecular identity of the specific protein on the erythrocyte membrane that reacts with respective CRPs, Western blotting was performed. A distinct protein corresponding to 220 kDa was detected on E_{TB} (Fig. 4f, lane 4) while a different set of CRP-binding molecules (270, 71 and 36 kDa) was observed on E_{VL} (lane 13) ($p<$ 0.001). In contrast, only a 149 kDa (lane 6 and 11) protein was observed on E_N reacting with CRP_{TB} and CRP_{VL} respectively. This common band was found on diseased-erythrocytes. No band was visible after reacting E_N with CRP_{Sigma} (lane 8). Membrane profile of E_{TB} (lane 3) and E_{VL} (lane 15) showed no band corresponding to purified CRPs (lane 2 and lane 16) indicating that CRP was not co-purified with erythrocyte membrane protein.

The binding of CRPs with the native structure of erythrocyte membrane proteins was checked by an immunoprecipitation experiment and analyzed by Western blotting. Immunocomplex of erythrocyte membrane proteins from TB that reacted with CRP_{TB} showed bands at 220 and 149 kDa (lane 5). Immunoprecipitated erythrocyte membrane proteins from VL after reacting with CRP_{VL} showed four proteins represented by 270, 149, 71 and 36 kDa bands (lane 14). Lane 7 and 12 corresponded to 149 kDa represented immunoprecipitated erythrocyte membrane proteins from normal reacting with CRP_{TB} and CRP_{VL} respectively. No band was detected after reacting erythrocyte membrane from normal individuals with CRP_{Sigma} (lane 9).

CRPs modulates membrane characteristics of diseased-erythrocytes

Enhanced binding of glycosylated CRPs with diseased-erythrocytes may be due to increased number of CRP-binding molecules on this membrane. In order to understand any alterations on the membrane due to this enhanced specific binding, membrane fragility, rigidity and hydrophobicity was investigated (Fig. 5).

a. Enhanced fragility due to binding with CRPs

At normal physiological saline concentration, only E_{TB} (n=10, Fig. 5a) and E_{VL} (n=10, Fig. 5b) were found to be 2.275±0.075 and 3.45±0.55-fold more fragile than E_N. After binding with corresponding CRP_{TB} and CRP_{VL}, additional 1.59±0.11 and 2.15±0.255-fold increase in fragility was observed in both E_{TB} and E_{VL} compared to unbound erythrocytes. Negligible differences in E_N were observed before and after binding with CRP_{TB} and CRP_{VL} (Fig. 5a,b). As expected, enhanced hemolysis is more pronounced at lower concentration (0.1–0.3%) of NaCl.

Fig. 4 Evaluation of binding of CRP to erythrocyte membrane protein. **a–d** *RBC-CRP binding by surface plasmon resonance (SPR)*. **a** Representative sensograms showing the result of the injection of varying concentrations (bottom to top curves: 10, 25, 40 and 50 μg/ml) of E_{TB} membrane protein as analyte, using flow buffer over a Biacore CM5 chip with covalently coupled CRP_{TB} (10 μg/ml) showing 2000 RU. Membrane proteins (150 μl) were injected in the running buffer at a flow rate of 30 μl /min. The detected binding is expressed in arbitrary resonance response (RU) as a function of time (s). **b** The interaction of membrane proteins from E_N (bottom to top curves: 10, 40 and 50 μg/ml) with immobilized CRP_{TB} was represented in different sensograms under identical condition as described in the Materials and Methods. Sensor chips CM5 were coated with CRP_{TB}. **c** Representative sensograms showing the result of the injection of varying concentrations (bottom to top curves: 10, 25, 40 and 50 μg/ml) of E_{VL} membrane protein as analyte, using flow buffer over covalently coupled CRP(-). **d** The interaction of membrane proteins from E_N (bottom to top curves: 10, 40 and 50 μg/ml) with immobilized CRP_{VL} was represented in different sensograms. **e** *By ELISA*. Equal amount of membrane proteins (2 μg/well/100 μl) from erythrocytes from TB was coated on wells separately, blocked, and different concentration of CRP_{TB} was allowed to bind in presence of PC and Ca^{+2} as described in Materials and Methods. The binding of CRP_{TB} with membrane protein from TB patient (-▣-) is shown. Similarly, the binding of CRP_{VL} with membrane protein from VL patient (-▥-) was determined. For comparison, normal erythrocyte membrane protein was coated similarly and binding with CRP_{TB} (- □ -) and CRP_{VL} (-▤-) was determined separately. Data are represented as mean ± SD from 5 experiments (p<0.0001) and normal individuals. **f** *SDS-PAGE, Western blotting and immunoprecipitation of erythrocyte membrane protein*. Erythrocyte membrane proteins (50 μg/lane) of patients and normal were electrophoresed on a 7.5% SDS-PAGE and transblotted onto nitrocellulose. The blots were incubated separately with purified respective CRP_{TB} and CRP_{VL} (5.0 μg)-PC-Ca^{+2} complex and probed with murine anti-human CRP antibodies followed by HRP-anti-murine IgG as described in Materials and Methods. Lane 1 and 17: Pre-stained broad range molecular weights marker. Lane 2 and 16: Purified CRP_{TB} and CRP_{VL} respectively. Lane 3, 10 and 15: Membrane proteins from erythrocytes of a representative TB patient, normal individual and VL patient were visualized by Coomassie stain. Lane 4: Western blotting of membrane proteins from erythrocytes of a representative TB patient with CRP_{TB}. Lane 6: Western blotting of membrane proteins from erythrocytes of a representative normal individual with CRP_{TB}. Lane 5 and 7: Immunoprecipitation of membrane proteins from erythrocytes of a representative TB patient and normal individual with CRP_{TB}. Lane 11 and 13: Western blotting of membrane proteins from erythrocytes of a normal individual and a VL patient with CRP_{VL} respectively. Lanes 12 and 14: Immunoprecipitation of membrane proteins from erythrocytes of a normal individual and a VL patient with CRP_{VL} respectively. Lane 8: Western blotting of membrane proteins from erythrocytes of a normal individual with CRP_{sigma} (S). Lane 9: Immunoprecipitation of membrane proteins from erythrocytes of a normal individual with CRP_{sigma} (S)

b. Decreased membrane rigidity of patients' erythrocytes

The erythrocytes from patients showed reduced membrane rigidity (r_s), the corresponding r_s values being 0.242± 0.001 for E_{TB} (n=5), and 0.246±0.002 for E_{VL} (n=5) as compared to 0.270±0.002 for E_N. Interestingly, after binding with CRP_{TB} and CRP_{VL}, rigidity of patients' erythrocytes was further decreased to 0.230±0.001 (E_{TB}) and 0.221± 0.003 (E_{VL}) as compared to only E_{TB} or E_{VL} (p<0.001). In

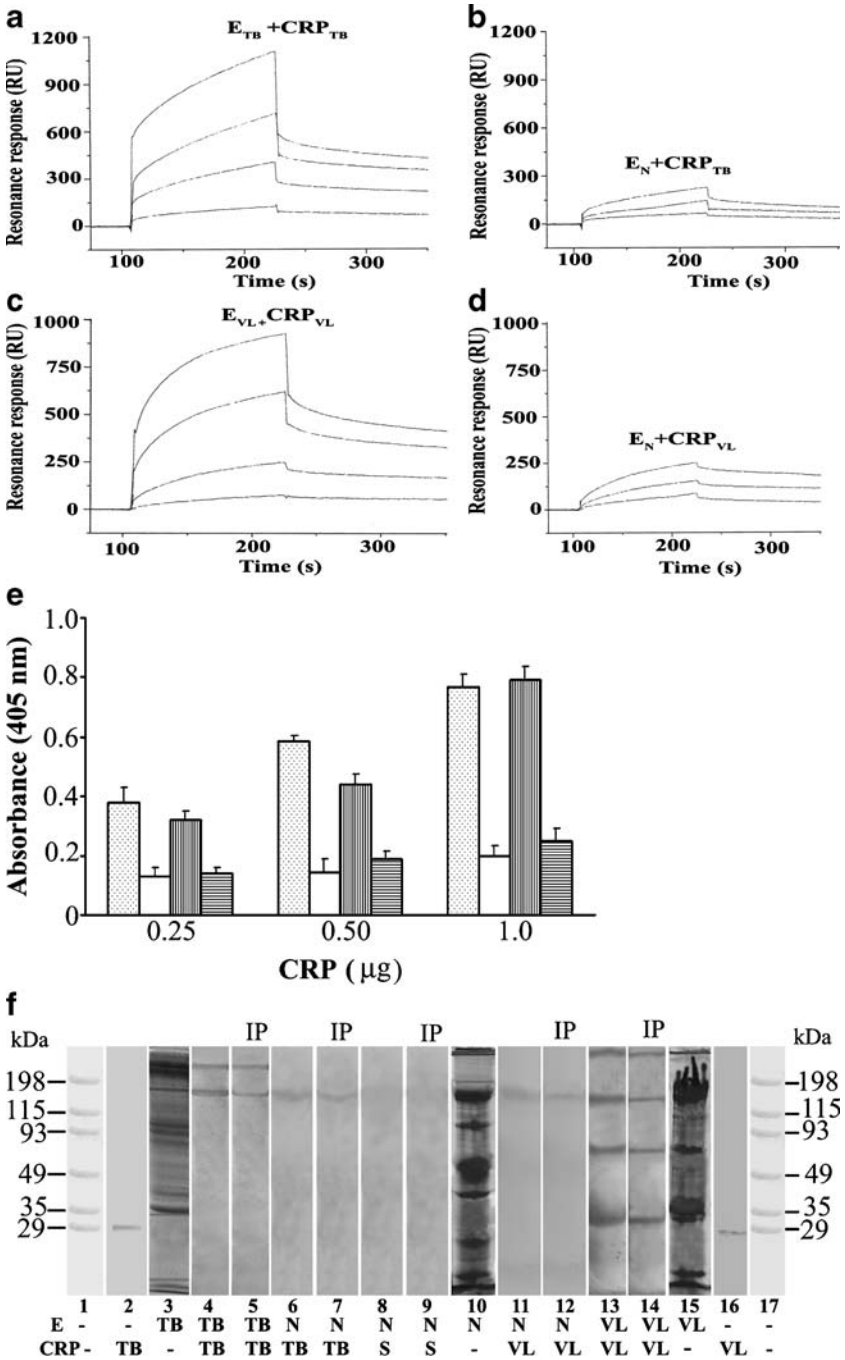

contrast, negligible change in rigidity was observed after binding of E_N with CRP_{TB} and CRP_{VL}; r_s being 0.268± 0.001 and 0.269±0.001 respectively.

c. Enhanced hydrophobicity due to binding of CRPs

Increased binding of ANS (arbitrary fluorescence intensity, Fig. 5c) to E_{TB} (15±2 a.u, curve 3) and E_{VL} (13±3 a. u, curve 4) indicated their enhanced hydrophobicity as compared to E_N (3±1 a.u, curve 6). After binding of patients' erythrocytes with respective CRPs, a drastic increase in ANS binding with E_{TB} (35±5 a.u, curve 2) and E_{VL} (45±6 a.u, curve 1) was observed. This observation clearly suggested the significant alteration in the hydrophobicity of patients' erythrocytes. In contrast, no significant alteration on E_N (8±2 a.u, curve 5) was observed, may be due to their negligible binding with CRP_{TB} and CRP_{VL}. Only ANS (2 a.u, curve 7) or buffer (1 a.u, curve 8) gave negligible binding. Due to the negligible binding of deglycosylated CRPs with respective erythrocyte, alterations in membrane parameters of $E_{TB/VL}$

was not in detectable range under the experimental conditions.

CRPs differentially triggered complement-cascade causing hemolysis

Enhanced osmofragility and hydrophobicity together with reduced membrane rigidity, as compared to E_N, indicated damage in the membrane of patients' erythrocytes. The binding of molecular variants of CRP with these erythrocytes showed further alteration in their membrane suggesting substantial damage in their membranes. Accordingly, the fate of this damaged-erythrocytes through complement-mediated hemolysis was investigated, using NHS as a source of complement (Fig. 6).

A dose-dependant increase in hemolysis of diseased-erythrocytes was observed with increase in the concentration of CRP using NHS (Fig. 6a). Interestingly, even at normal physiological CRP concentration (10 μg/ml), CRP_{TB} and CRP_{VL} triggered 72±3% and 81±5% hemolysis of E_{TB} and E_{VL} respectively. This was nearly 4.085±0.20 and 6.20± 0.42-fold higher than hemolysis of E_N (Fig. 6a, $p<0.001$).

Deglycosylated CRP_{TB} and CRP_{VL} showed very negligible hemolysis (%) *i.e* 6±3 % (E_{TB}) and 4±2% (E_{VL}) respectively as binding of deglycosylated CRPs with erythrocytes were very low. This again re-confirmed that glycosylation pose a pivotal role in this binding. Lysis (%) of E_N triggered by CRP_{TB} and CRP_{VL} was minimal (2±1%) (Fig. 6b). Comparable lysis was observed using patients' serum, CRP-depleted serum, patients' serum and NHS as sources of complement, signifying the *in vivo* scenario (Fig. 6b). As CRP-mediated complement-activation requires Ca^{+2}, CRP and NHS, addition of EDTA or anti-CRP antibodies or decomplemented serum caused complete abolition of hemolysis. Human CRP did not interact with guinea pig C1q [37] and addition of guinea pig sera induced no complement-activation (< 2%, not shown).

Discussion

CRP is a multifunctional protein [3, 38]. It has the ability to bind to ligands like polymorphonuclear leukocytes; macrophage etc, and finally activates the classical complement

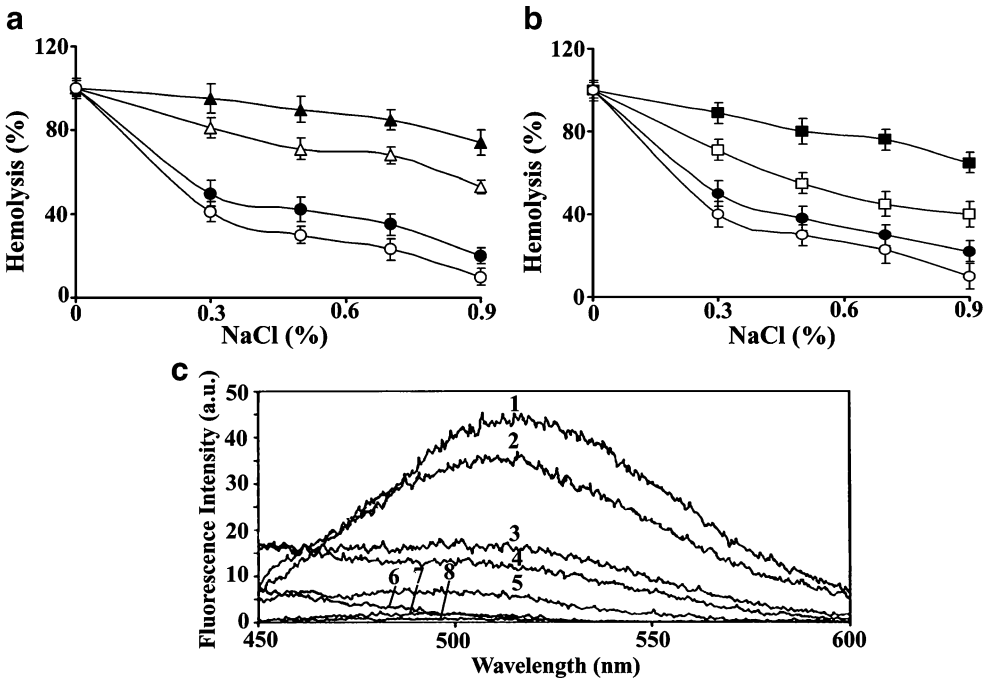

Fig. 5 Altered erythrocyte membranes in diseased conditions. *Hemolysis (%) of erythrocytes*. Osmotic fragility was determined as described in Materials and Methods and data are representative of five experiments as mean ± SD. **a** The hemolysis (%) of E_{TB} before (-△-) and after (-▲-) binding with CRP_{TB} and corresponding values of E_N before (-○-) after binding (-●-) with CRP_{TB} are shown at various NaCl concentrations (%). **b** In parallel, the % of hemolysis of E_{VL} in absence (-□-) and presence of CRP_{VL} (-■-) and corresponding values of E_N before (-○-) after binding (-●-) with CRP_{VL} are shown. **c** *Induced hydrophobicity of diseased-erythrocytes*. Washed E_{TB}, E_{VL} and E_N (1×10^9) were separately incubated initially for 1 hr at 0°C with respective CRP_{TB}-PC-Ca^{+2} or CRP_{VL}-PC-Ca^{+2} complex (5.0 μg), washed and further incubated with ANS at 37°C. Fluorescence spectra were recorded as described in Material and Methods. Binding of ANS has shown in arbitrary fluorescence intensity, a.u. Curve 1: binding of E_{VL} with CRP_{VL}. curve 2: binding of E_{TB} with CRP_{TB}. curve 3: E_{TB}. curve 4: E_{VL}. curve 5: Normal erythrocytes after binding with CRP. curve 6: Normal Erythrocytes. Only ANS (curve 7) and buffer (curve 8) showed negligible binding

pathway [37]. CRP binds to damaged or necrotic cells [39–41], presumably through exposed membrane PC moieties. The reactivity of CRPs is mainly due to its association with varieties of ligands [42], therefore, a search for the identification of more physiological ligands may be useful in understanding the function of CRPs during infections and inflammatory conditions [43].

The main aim of this study was to investigate the role of glycosylated CRP in the clearance of diseased-erythrocytes. Although, we had earlier reported, the role of CRP in complement-mediated hemolysis in malaria [44, 45], however, the direct involvement of glycosylation in CRP for causing hemolysis has not yet been demonstrated. Accordingly, in this report, we have systematically investigated two other related diseases, where anemia is manifested. We have shown that (i) distinct molecular variants of glycosylated CRP_{TB} and CRP_{VL} (Fig. 1a) binds 3.16±0.325-fold more to diseased-erythrocytes as compared to normal (Figs. 2, 3 and 4), (ii) presence of distinct disease-associated CRP-binding molecules on erythrocytes (Fig. 4f) and the density of CRP-binding molecules was 1000 –10,000-fold more as compared to E_N (Fig. 3), (iii) binding of patients' erythrocytes with CRP_{TB} and CRP_{VL} showed alteration in the membrane fragility, fluidity and hydrophobicity (Fig. 5) and (iv) this binding leads to hemolysis via complement activation (Fig. 6). Taken together, it may be envisaged that this could be one of the probable mechanisms explaining the characteristic anemia in TB and VL. Interestingly, the binding of erythrocytes of malaria with disease-associated CRP purified from malaria patients also showed similar trend of binding, alteration in membrane parameters and complement-triggered lysis [44, 45]. Thus the pathophysiological mechanism of such removal of damaged-erythrocytes from patient's blood by CRP may be a general phenomenon at least in case of malaria, TB and VL and demonstrating a potential effector-function of CRP.

Our results strongly suggest that small but significant variations in CRP_{TB} and CRP_{VL} at the molecular level may occur possibly due to the variations in carbohydrate compositions (Fig. 1; Table 2) as reported earlier (7–9). The differential presence of carbohydrates in these two CRPs is demonstrated by various approaches. The binding with several lectins (Fig. 1b,c, Table 2), an increase in pI after deglycosylation (Fig. 1g); decrease in molecular weight after treatment with sialidase followed by *N*-glycosidase F enzyme (Fig. 1f), also GLC and MALDI-TOF demonstrated the existence of variations in glycosylation (Fig. 1d,e). The decrease in molecular mass after *N*-glycosidase F-digestion confirmed the presence of *N*-linked glycosylation (Fig. 1f). The oligosaccharides of these CRPs are mainly composed of mannose, galactose, glucose and sialic acid (Fig. 1c–e, Table 2). The presence of other sugars may be negligible as they were undetectable by GLC under this experimental condition. The presence of sialic acid in CRP was further confirmed by MALDI-TOF and also its reactivity with sialic acid binding lectins (Table 2). Increase in pI after sialidase treatment also hinted for the presence of charged sugar [8].

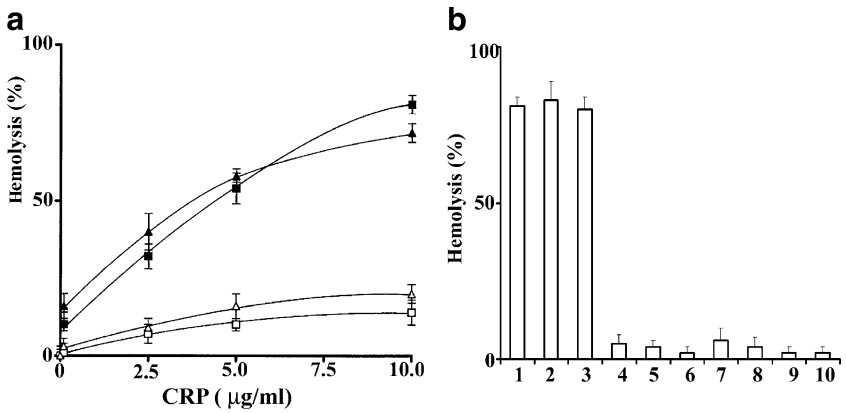

Fig. 6 Complement-mediated lysis of diseased-erythrocytes. **a** *Dose-dependant lysis of erythrocytes as induced by CRPs*. CRP_{TB} and CRP_{VL} (0.1–10 μg/ml) was allowed to bind with E_{TB}, E_{VL} and E_N separately in presence of PC and Ca^{+2} followed by addition of normal human serum (NHS), as a source of complement. Dose-dependent lysis (%) of E_{TB} (-▲-) and E_{VL} (-■-), after binding with CRP_{VL} and CRP_{TB} are shown respectively. In contrast, lysis (%) of E_N after binding with CRP_{TB} (-△-) and CRP_{VL} (-□-) was minimum. Each point is the average of triplicate determination. **b** *Comparative analysis of complement-lysis*. At fixed concentration of CRP (10.0 μg/ml), hemolysis (%) of patients' erythrocytes was compared separately using sera either from (1) normal individuals, (2) patients, (3) CRP depleted patient's serum and (4) decomplemented NHS as sources of complement. Pre-incubation of reaction mixture with (5) EDTA (10 mM) and (6) murine anti-CRP antibodies negligibly reduced this hemolysis (%). Deglycosylated CRP_{TB} and CRP_{VL} (10 μg/ml) were similarly allowed to bind with E_{TB}, E_{VL} and E_N separately in presence of PC and Ca^{+2} followed by addition of normal human serum (NHS), as a source of complement. Lysis (%) of E_{TB} with CRP_{TB} (7), E_{VL} with CRP_{VL} (8), E_N with CRP_{TB} (9), and E_N with CRP_{VL} (10) are represented respectively. Results are expressed as mean of ± SD of data from 4–5 separate experiments

These sialic acids are predominantly α2–3-linked. Based on these observations, it may be reasonable to conclude that WGA binding with CRP is preferentially through Neu5Ac. Additionally, under the experimental condition, no peak for *N*-acetylhexoamines was observed both in GLC and MALDI-TOF may be due to either absence or the presence of negligible amount of this sugar compared to predominance of other three hexoses. UEA binding revealed the differential presence of fucose (Table 2). Absence of detectable peak in GLC, no shift in pI and electrophoretic mobility before and after deglycosylation clearly suggested that CRP_{Sigma} is non-glycosylated.

Sialic acids play a major role in different molecular and cellular reactions [28, 46–49]. The acuteness of a disease may be reflected from the levels of sialic acids thus it may be crucial in combating various causative agents. Therefore, it may be envisaged that in different diseases the sialic acid content of human CRP may be a key determinant in combating various inducing agents. Small variations in the pI (8.5–9.8) of CRPs (Fig. 1g) possibly occur due to the net donation of charged sugars like sialic acids. Although such variation in pI of CRP in plasma of various diseases is known [8, 45, 50, 51], the cause of such differences is not investigated in detail.

The induction of such distinct chemical entities at the molecular level has previously been established in our laboratory [7–9, 44–50, 52–56]. Both glycosylated and deglycosylated CRP retained their native structure as well as their calcium-dependant PC binding property and potential to bind with Sepharose-PC. Considering the purification procedure, the presence of non-covalently bound sugars is highly unlikely confirming induction of glycosylation in TB and VL. The *in vivo* existence of glycosylated CRP could be explained due to possible induction of some glycosyltransferases, which may facilitate differential level of glycosylation as a part of post-translational modification of CRP. Therefore, it is possible that minute changes in glycosylation make these two CRPs differ chemically. However, these small changes in CRP molecule are possibly crucial for specific biological functions *in vivo* [8].

The differential lectin-like behaviour, sugar-binding properties and immunological reactivity of invertebrates [57], fish [53–55] and human CRPs [16] suggested minute variations in their structures leading in their possible altered functions in diseased conditions. The precise outcome of this glycosylation is still an open-ended question. However, such induction of glycosylation in CRPs may affect its binding reactivity towards histones, chromatin, ribonucleoprotein particles and pathogens or may alter its biological functions like agglutination, activation of the complement cascade. It is possible that there is necessity for induction of such molecular variants of CRP for their proper binding and successful detoxification of detrimental substances that enter into the circulation.

Glycosylation appears to be a critical determinant in facilitating erythrocyte-CRP binding in the presence of calcium and PC (Figs. 2, 3 and 4). The specificity of this interaction was reconfirmed by inhibition of binding in presence of excess cold CRP (Fig. 2b, 3a,b). Loss of binding of deglycosylated CRP with erythrocytes again highlighted the significant role of glycosylation induced in these CRPs (Fig. 2b).

Scatchard analysis suggested the differential and specific binding of patients' erythrocyte-CRP with an enhanced receptor-density as compared to much lower receptor-densities on normal (Fig. 3). This observation was further corroborated by SPR analysis wherein a significant difference was observed between the RU values of patients' erythrocytes and normal erythrocytes after binding with CRP (Fig. 4a–d). Differences in the number of specific molecules on E_{TB} and E_{VL} having affinity towards CRP also implied the differences in CRP_{TB} and CRP_{VL} (Fig. 4f). Due to glycosylation, some specific molecules are induced on patient's erythrocytes that differentially reacted with patient's CRP. Thus disease-associated binding was observed as compared to normal, although, a few binding sites of the erythrocytes may possibly be blocked by CRP present in patient's serum *in vivo*. However, the amount of bound CRP may possibly be very low as evident by many of our approaches described here. No co-purified CRPs were visible in SDS-PAGE membrane profile of purified erythrocytes (Fig. 4f, lane 3, 15).

Based on their molecular weight, it may be envisaged that the newly identified CRP-target molecules on erythrocyte surface are unique and different from the already reported complement receptor 1 (CR1), decay-accelerating factor (DAF, CD55), and CD59 molecules [45]. Reports have revealed a different mechanism of erythrocyte clearance through liver and spleen [58, 59].

Membrane destabilization of erythrocytes has earlier been reported in VL, malaria and leukemia patients [45, 60–62]. In this study, patient's erythrocytes revealed altered fragility, fluidity, hydrophobicity indicating damage in membrane, which was further altered due to binding with CRPs. This membrane destabilization could be due to the lectin-like behaviour of CRP [16, 45]. Thus CRP when added exogenously will cross-link with the membrane surface receptors leading to lateral molecular reorganizations in the plane of the bilayer [63–65].

This molecular reorganization thus, possibly exposes PC, the ligand for erythrocyte-CRP binding on the outer leaflet of bilayer. However, physiological level of PC and Ca^{+2} were added to facilitate erythrocyte-CRP binding *in vitro*. This erythrocyte-CRP binding might thus activate the complement mediated-hemolysis in TB

and VL and this could cause formation of membrane leaks [63–67].

In presence of calcium and PC, erythrocyte are known to bind with the 'recognition face' of pentameric CRP [3, 22] and this activates the complement-cascade possibly *via* C1q recognition [3, 68] on the 'opposite face' of CRP. Mutational analysis has revealed that Asp^{112} and Tyr^{175} are the major determinants and important contact residues for C1q binding to complexed CRP [69] while Asn158, did not cause significant changes in C1q binding. Asn158 is the reported site of *N*-glycosylation on CRP molecule [8]. Therefore, C1q binding site (Asp^{112} and Tyr^{175}) and receptor binding site (Asn158) on glycosylated CRP is non-overlapping. This hinted towards the notion that glycosylated CRP complex may be capable of binding to C1q finally and thus activating the complement pathway. The critical role of glycosylation in activating the classical and alternate complement pathway has previously been demonstrated from our laboratory [70–72]. This study further substantiates this concept. The observed hemolysis in our studies confirmed that CRP-mediated complement-activation ends with consumption of terminal membrane attack complex (MAC). Though most of the reported CRP-mediated complement-activation is essentially limited to stage involving C1–C4 [73] some reports also suggested deposition of MAC by CRP [40, 74]. Therefore, our results are consistent with these reports revealing CRP-complement activation by binding with erythrocyte-CRP.

Induction of glycosylation in CRP is possibly essential for endorsing the lysis of damaged-erythrocytes. CRP essentially favours the host and hence maintains homeostasis in these diseases. In conclusion, our work provides experimental evidences of the ability of disease-associated CRP to trigger efficient complement-pathway suggesting one of the alternative mechanisms for hemolysis causing anemia in TB and VL.

Acknowledgement This work was supported by the Council of Scientific and Industrial Research (CSIR), I.I.C.B, Department of Science and Technology and the Indian Council of Medical Research, Govt. of India. W.A and S.M receive their Senior Research fellowships from CSIR; S.B from University Grants Commission. We are thankful to Sajal Samanta and Biswajit Khatua; Suchandra Chowdhury, Kaushik Bhattacharya for FACS; Asish Mallick for their help; Samir Roy for SPR and Sandip Chakrabarty for MALDI-TOF analysis.

References

1. Agrawal, A.: CRP after 2004. Mol. Immunol. **42**, 927–930 (2005). doi:10.1016/j.molimm.2004.09.028
2. Marnell, L., Mold, C., Du Clos, T.W.: C-reactive protein: ligands, receptors and role in inflammation. Clin. Immunol. **117**, 104–111 (2005). doi:10.1016/j.clim.2005.08.004
3. Volanakis, J.E.: Human C-reactive protein: expression, structure, and function. Mol. Immunol. **38**, 189–197 (2001). doi:10.1016/S0161-5890(01)00042-6
4. Gould, J.M., Weiser, J.N.: Expression of C-reactive protein in the human respiratory tract. Infect. Immun. **69**, 1747–1754 (2001). doi:10.1128/IAI.69.3.1747-1754.2001
5. Jabs, W.J., Logering, B.A., Gerke, P., Kreft, B., Wolber, E.M., Klinger, M.H., Fricke, L., Steinhoff, J.: The kidney as a second site of human C-reactive protein formation *in vivo*. Eur. J. Immunol. **33**, 152–161 (2003). doi:10.1002/immu.200390018
6. Volanakis, J.E., Kaplan, M.H.: Specificity of C-reactive protein for choline phosphate residues of pneumococcal C-polysaccharide. Proc. Soc. Exp. Biol. Med. **136**, 612–614 (1971)
7. Das, T., Mandal, C., Mandal, C.: Protein A-a new ligand for human C-reactive protein. FEBS Lett. **576**, 107–113 (2004). doi:10.1016/j.febslet.2004.08.072
8. Das, T., Sen, A., Kempf, T., Pramanik, S.R., Mandal, C., Mandal, C.: Induction of glycosylation in human C-reactive protein under different pathological conditions. Biochem. J. **373**, 345–355 (2003). doi:10.1042/BJ20021701
9. Das, T., Mandal, C., Mandal, C.: Variations in binding characteristics of glycosylated human C-reactive proteins in different pathological conditions. Glycoconj. J. **20**, 537–543 (2004). doi:10.1023/B:GLYC.0000043290.90182.e6
10. Du Clos, T.W., Marnell, L., Zlock, L.R., Burlingame, R.W.: Analysis of the binding of C-reactive protein to chromatin subunits. J. Immunol. **146**, 1220–1225 (1991)
11. Du Clos, T.W., Zlock, L.T., Marnell, L.: Definition of a C-reactive protein binding determinant on histones. J. Biol. Chem. **266**, 2167–2171 (1991)
12. James, K., Hansen, B., Gewurz, H.: Binding of C-reactive protein to human lymphocytes. II. Interaction with a subset of cells bearing the Fc receptor. J. Immunol. **127**, 2545–2550 (1981)
13. Gewurz, H., Mold, C., Siegel, J., Fiedel, B.: C-reactive protein and the acute phase response. Adv. Intern. Med. **27**, 345–372 (1982)
14. Kaplan, M.H., Volanakis, J.E.: Interaction of C-reactive protein complexes with the complement system. I. Consumption of human complement associated with the reaction of C-reactive protein with pneumococcal C-polysaccharide and with the choline phosphatides, lecithin and sphingomyelin. J. Immunol. **112**, 2135–2147 (1974)
15. McGrath, F.D., Brouwer, M.C., Arlaud, G.J., Daha, M.R., Hack, C.E., Roos, A.: Evidence that complement protein C1q interacts with C-reactive protein through its globular head region. J. Immunol. **176**, 2950–2957 (2006)
16. Kottgen, E., Hell, B., Kage, A., Tauber, R.: Lectin specificity and binding characteristics of human C-reactive protein. J. Immunol. **149**, 445–453 (1992)
17. Arese, P., Turrini, F., Schwarzer, E.: Band 3/complement-mediated recognition and removal of normally senescent and pathological human erythrocytes. Cell. Physiol. Biochem. **16**, 133–146 (2005). doi:10.1159/000089839
18. Lutz, H.U.: Innate immune and non-immune mediators of erythrocyte clearance. Cell Mol Biol Noisy-le-grand **50**, 107–116 (2004)
19. Volanakis, J.E., Clements, W.L., Schrohenlohr, R.E.: C-reactive protein: purification by affinity chromatography and physiochemical characterization. J. Immunol. Methods **23**, 285–295 (1978). doi:10.1016/0022-1759(78)90203-X
20. Christner, R.B., Mortensen, R.F.: Specificity of the binding interaction between human serum amyloid P-component and immobilized human C-reactive protein. J. Biol. Chem. **269**, 9760–9766 (1994)
21. Lowry, O.H., Rosebrough, N.J., Farr, A.L., Randall, R.J.: Protein measurement with the Folin phenol reagent. J. Biol. Chem. **193**, 265–275 (1951)

22. Thompson, D., Pepys, M.B., Wood, S.P.: The physiological structure of human C-reactive protein and its complex with phosphocholine. Structure **7**, 169–177 (1999). doi:10.1016/S0969-2126(99)80023-9
23. Laemmli, U.K.: Cleavage of structural proteins during the assembly of the head of bacteriophage T4. Nature **227**, 680–685 (1970). doi:10.1038/227680a0
24. Towbin, H., Staehelin, T., Gordon, J.: Electrophoretic transfer of proteins from polyacrylamide gels to nitrocellulose sheets: procedure and some applications. Proc. Natl. Acad. Sci. USA **76**, 4350–4354 (1979). doi:10.1073/pnas.76.9.4350
25. Hunter, W.M.: Handbook of experimental medicine, Weir, D.M. edition, Blackwell Scientific Publication, Oxford, **14.1–14.3** (1978)
26. Sloneker, J.H.: Gas-liquid chromatography of alditol acetates, methods in carbohydrate chemistry. In: Whistler, R.L., BeMiller, J.N. (eds.) Academic Press Inc., **VI**, 20–24 (1972)
27. Lönngren, J., Svensson, S.: Mass spectrometry in structural analysis of natural carbohydrates. Adv. Carbohydr. Chem. Biochem. **29**, 41–106 (1974). doi:10.1016/S0065-2318(08)60248-6
28. Pal, S., Chatterjee, M., Bhattacharya, D.K., Bandhyopadhyay, S., Mandal, C.: Identification and purification of cytolytic antibodies directed against O-acetylated sialic acid in childhood acute lymphoblastic leukemia. Glycobiology **10**, 539–549 (2000). doi:10.1093/glycob/10.6.539
29. O' Farrell, P.Z., Goodman, H.M., O' Farrell, P.Z.: High resolution two-dimensional electrophoresis of basic as well as acidic proteins. Cell **12**, 1133–1141 (1977). doi:10.1016/0092-8674(77)90176-3
30. Coligan E.J., Kruisbeek M.A., Margulies H.D., Shevach M.E., Strober W.: Current protocols in immunology (Wiley Interscience, National Institute of Health, 1993), 32–34 (1993)
31. Scatchard, G.: The attractions of proteins for small molecules and ions. Ann. N. Y. Acad. Sci. **51**, 660–672 (1949). doi:10.1111/j.1749-6632.1949.tb27297.x
32. Shukla, A.K., Schauer, R.: Fluorimetric determination of unsubstituted and 9(8)-O-acetylated sialic acids in erythrocyte membranes. Hoppe Seylers Z. Physiol. Chem. **363**, 255–262 (1982)
33. Sharma, V., Chatterjee, M., Mandal, C., Sen, S., Basu, D.: Rapid diagnosis of Indian visceral leishmaniasis using achatinin H, a 9-O-acetylated sialic acid binding lectin. Am. J. Trop. Med. Hyg. **58**, 551–554 (1998)
34. Ghosh, S., Bandyopadhyay, S., Bhattacharya, D.K., Mandal, C.: Altered erythrocyte membrane characteristics during anemia in childhood acute lymphoblastic leukemia. Ann. Hematol. **84**, 76–84 (2005). doi:10.1007/s00277-004-0933-0
35. Osmand, A.P., Mortensen, R.F., Siegel, J., Gewurz, H.: Interactions of C-reactive protein with the complement system. III. Complement-dependent passive hemolysis initiated by CRP. J. Exp. Med. **142**, 1065–1077 (1975). doi:10.1084/jem.142.5.1065
36. David, M., Pepys, M.B., Hawkins, P.N.: Metabolic and scintigraphic studies of radioiodinated human C-reactive protein in health and diseases. J. Clin. Invest. **91**, 1351–1357 (1993). doi:10.1172/JCI116336
37. Volanakis, J.E., Kaplan, M.H.: Interaction of C-reactive protein complexes with the complement system. II. Consumption of guinea pig complement by CRP complexes: requirement for human C1q. J. Immunol. **113**, 9–17 (1974)
38. Gabay, C., Kushner, I.: Acute-phase proteins and other systemic responses to inflammation. N. Engl. J. Med. **340**, 448–454 (1999). doi:10.1056/NEJM199902113400607
39. Kushner, I., Rakita, L., Kaplan, M.H.: Studies of acute-phase protein. II. Localization of Cx-reactive protein in heart in induced myocardial infarction in rabbits. J. Clin. Invest. **42**, 286–292 (1963). doi:10.1172/JCI104715
40. Li, P., Mold, C., Du Clos, T.W.: Sublytic complement attack exposes C-reactive protein binding sites on cell membranes. J. Immunol. **152**, 2995–3005 (1994)
41. Narkates, A.J., Volanakis, J.E.: C-reactive protein binding specificities: artificial and natural phospholipid bilayers. Ann. N. Y. Acad. Sci. **389**, 172–182 (1982). doi:10.1111/j.1749-6632.1982.tb22135.x
42. Pepys, M.B., Baltz, M.L.: Acute phase proteins with special reference to C-reactive protein and related proteins (pentaxins) and serum amyloid A protein. Adv. Immunol. **34**, 141–212 (1983). doi:10.1016/S0065-2776(08)60379-X
43. Pepys, M.B.: C-reactive protein fifty years on. Lancet **1**, 653–657 (1981). doi:10.1016/S0140-6736(81)91565-8
44. Ansar, W., Bandyopadhyay, S.M., Chowdhury, S., Habib, S.H., Mandal, C.: Role of C-reactive protein in complement-mediated hemolysis in Malaria. Glycoconj. J. **23**, 233–240 (2006). doi:10.1007/s10719-006-7928-0
45. Ansar, W., Mandal, C., Habib, S.K.H., Roy, S., Mandal, C.: Unraveling the C-reactive protein complement-cascade in destruction of red blood cells: potential pathological implications in *Plasmodium falciparum* malaria. Cell. Physiol. Biochem. **23**, 175–190 (2009). doi:10.1159/000204106
46. Paul, I., Mandal, C., Allen, A.K., Mandal, C.: Molecular variants of C-reactive proteins from the major carp Catla catla in fresh and polluted aquatic environments. Glycoconj. J. **18**, 547–556 (2001). doi:10.1023/A:1019696430477
47. Mandal, C., Chatterjee, M., Sinha, D.: Investigation of 9-O-acetylated sialoglycoconjugates in childhood acute lymphoblastic leukaemia. Br. J. Haematol. **110**, 801–812 (2000). doi:10.1046/j.1365-2141.2000.02105.x
48. Sinha, D., Chatterjee, M., Mandal, C.: O-acetylation of sialic acids-their detection, biological significance and alteration in diseases. Trends Glycosci. Glycotechnol. **12**, 17–33 (2000)
49. Sinha, D., Mandal, C., Bhattacharya, D.K.: Identification of 9-O acetyl sialoglycoconjugates (9-OAcSGs) as biomarkers in childhood acute lymphoblastic leukemia using a lectin, AchatininH, as a probe. Leukemia **13**, 119–125 (1999). doi:10.1038/sj.leu. 2401312
50. Mandal, C., Biswas, M., Nagpurkar, A., Mookerjea, S.: Isolation of a phosphoryl choline-binding protein from the hemolymph of the snail, Achatina fulica. Dev. Comp. Immunol. **15**, 227–239 (1991). doi:10.1016/0145-305X(91)90016-R
51. Lasson, A., Goransson, J.: No microheterogenous changes of plasma C-reactive protein found in man during various diseases. Scand. J. Clin. Lab. Invest. **59**, 293–304 (1999). doi:10.1080/00365519950185661
52. Mandal, C., Srinivasan, G.V., Chowdhury, S., Chandra, S., Mandal, C., Schauer, R., Mandal, C.: High level of sialate-O-acetyltransferase activity in lymphoblasts of childhood acute lymphoblastic leukaemia (ALL): enzyme characterization and correlation with disease status. Glycoconj. J. **26**, 57–73 (2009). doi:10.1007/s10719-008-9163-3
53. Sinha, S., Mandal, C.: Microheterogeneity of C-reactive protein in the sera of fish Labeo rohita induced by metal pollutants. Biochem. Biophys. Res. Commun. **226**, 681–687 (1996). doi:10.1006/bbrc.1996.1414
54. Sinha, S., Mandal, C.N., Allen, A.K., Mandal, C.: Acute phase response of C-reactive protein of Labeo rohita to aquatic pollutants is accompanied by the appearance of distinct molecular forms. Arch. Biochem. Biophys. **369**, 139–150 (2001). doi:10.1006/abbi.2001.2592
55. Paul, I., Mandal, C., Mandal, C.: Effect of environmental pollutants on the C-reactive protein of a freshwater major carp, Catla catla. Dev. Comp. Immunol. **22**, 519–532 (1998). doi:10.1016/S0145-305X(98)00031-7
56. Chatterjee, M., Sharma, V., Sundar, S., Sen, S., Mandal, C.: Identification of antibodies directed against O-acetylated sialic acids in visceral leishmaniasis: its diagnostic and prognostic role. Glycoconj. J. **15**, 1141–1147 (1998). doi:10.1023/A:1006963806318

57. Baltz, M.L., De Beer, F.C., Feinstein, A., Munn, E.A., Fletcher, T. C., Taylor, J., Bruton, C., Clamp, J.R., Davies, A.J.S., Pepys, M. B.: Phylogenetic aspects of C-reactive protein and related protein. Ann. N. Y. Acad. Sci. **389**, 49–75 (1982). doi:10.1111/j.1749-6632.1982.tb22125.x
58. Mold, C., Gurulé, C., Otero, D., Du Clos, T.W.: Complement-dependent binding of C-reactive protein complexes to human erythrocyte CR1. Clin. Immunol. Immunopathol. **8**, 153–160 (1996). doi:10.1006/clin.1996.0171
59. Davies, K.A., Hird, V., Stewart, S., Sivolapenko, G.B., Jose, P., Epenetos, A.A., Walport, M.J.: A study of *in vivo* immune complex formation and clearance in man. J. Immunol. **144**, 4613–4620 (1990)
60. Kundu, M., Basu, J., Chakrabarti, P.: Chronic myelogenous leukemia: alterations in red cell membrane band 3 and increased IgG binding. Indian J. Biochem. Biophys. **27**, 456–459 (1990)
61. Roy, S.S., Sen, G., Biswas, T.: Role of sulfhydryl groups in band 3 in the inhibition of phosphate transport across erythrocyte membrane in visceral leishmaniasis. Arch. Biochem. Biophys. **436**, 121–127 (2005). doi:10.1016/j.abb.2005.01.015
62. Mukherjee, K., Chowdhury, S., Mondal, S., Mandal, C., Chandra, S., Bhadra, R.K., Mandal, C.: 9-O-acetylated GD3 triggers programmed cell death in mature erythrocytes. Biochem. Biophys. Res. Commun. **362**, 651–657 (2007). doi:10.1016/j.bbrc.2007.08.048
63. Gupta, R.K., Pande, A.H., Gulla, K.C., Gabius, H.J., Hajela, K.: Carbohydrate-induced modulation of cell membrane. VIII. Agglutination with mammalian lectin galectin-1 increases osmofragility and membrane fluidity of trypsinized erythrocytes. FEBS Lett. **580**, 1691–1695 (2006). doi:10.1016/j.febslet.2006.02.006
64. Pande, A.H., Sumati, N., Hajela, N., Hajela, K.: Carbohydrate induced modulation of cell membrane VII. Binding of exogenous lectin increases osmofragility of erythrocytes. FEBS Lett. **427**, 21–24 (1998). doi:10.1016/S0014-5793(98)00384-6
65. Hajela, K., Pande, A.H., Sumati, N.: Carbohydrate induced modulation of cell membrane. VI. Binding of exogenous lectin induces susceptibility of erythrocytes to free radical damage: a spin label study. FEBS Lett. **406**, 255–258 (1997). doi:10.1016/S0014-5793(97)00272-X
66. Volanakis, J.E., Wirtz, K.W.: Interaction of C-reactive protein with artificial phosphatidylcholine bilayers. Nature **281**, 155–157 (1979). doi:10.1038/281155a0
67. Deuticke, B., Lutkemeier, P., Sistemich, M.: Ion selectivity of aqueous leaks induced in the erythrocyte membrane by cross linking of membrane proteins. Biochim. Biophys. Acta **775**, 150–160 (1984). doi:10.1016/0005-2736(84)90165-2
68. Agrawal, A., Volanakis, J.E.: Probing the C1q-binding site on human C-reactive protein by site-directed mutagenesis. J. Immunol. **152**, 5404–5410 (1994)
69. Agrawal, A., Shrive, A.K., Greenhough, T.J., Volanakis, J.E.: Topology and structure of the C1q-binding site on C-reactive protein. J. Immunol. **166**, 3998–4004 (2001)
70. Chava, A.K., Chatterjee, M., Sharma, V., Sundar, S., Mandal, C.: Variable degree of alternative complement pathway-mediated hemolysis in Indian visceral leishmaniasis induced by differential expression of 9-O-acetylated sialoglycans. J. Infect. Dis. **189**, 1257–1264 (2004). doi:10.1086/382752
71. Bandyopadhyay, S., Chatterjee, M., Das, T., Bandyopadhyay, S., Sundar, S., Mandal, C.: Antibodies directed against O-acetylated sialoglycoconjugates accelerate complement activation in Leishmania donovani promastigotes. J. Infect. Dis. **190**, 2010–2019 (2004). doi:10.1086/425519
72. Sharma, V., Chatterjee, M., Sen, G., Kumar, C.A., Mandal, C.: Role of linkage specific 9-O-acetylated sialoglycoconjugates in activation of the alternate complement pathway in mammalian erythrocytes. Glycoconj. J. **17**, 887–893 (2000). doi:10.1023/A:1010925414222
73. Berman, S., Gewurz, H., Mold, C.: Binding of C-reactive protein to nucleated cells leads to complement activation without cytolysis. J. Immunol. **136**, 1354–1359 (1986)
74. Klegeris, A., Singh, E.A., McGeer, P.L.: Effects of C-reactive protein and pentosan polysulphate on human complement activation. Immunology **106**, 381–388 (2002). doi:10.1046/j.1365-2567.2002.01425.x